# Spatial and temporal dynamics of bird movement over the North Sea

Jens van Erp, Judy Shamoun-Baranes

University of Amsterdam, Institute for Biodiversity and Ecosystem Dynamics, PO Box 94240, 1090GE Amsterdam

Main Author: Jens van Erp

Project leader: Judy Shamoun-Baranes

Report number: 03-266

Date of publication: Januari 2024


Commissioned by: Gemini wind park

Contact: Luuk Folkerts

Report should be cited as:

Van Erp JA, Shamoun-Baranes J 2024. Spatial and temporal dynamics of bird movement over the North Sea. Report No. 03-266. University of Amsterdam. Doi: 10.21942/uva.25021793

# Table of contents

Table of contents 2
1. Introduction 3
1.1 Background 3
1.2 Aims of this report 5
2. Monitoring infrastructure 6
2.1 Radar monitoring 6
2.2 Data flow & responsible parties 7
3. Radar data 9
3.1 Data structure 9
3.2 Accessibility 10
3.3 Post-processing 11
4. Patterns of bird flight 17
4.1 Bird abundance throughout the seasons 17
4.2 Daily patterns of bird flight throughout the seasons 22
5. Migration in spring and autumn 24
6. Radar validation 27
7. Conclusions 28
8. Research outcomes 30
Acknowledgements 31
Funding 31
Appendices 31
References 32
Supplementary material 33

# 1. Introduction

## 1.1 Background

Gemini offshore wind farm is located in the Dutch part of the North Sea, 85 km north of the coast of Groningen, 60 km north of the island Schiermonnikoog (Fig. 1). The Gemini wind farm consists of 150 wind turbines, totalling 600 MW and two offshore high voltage stations. Start of construction was mid-2015. Gemini is fully operational since 2017.

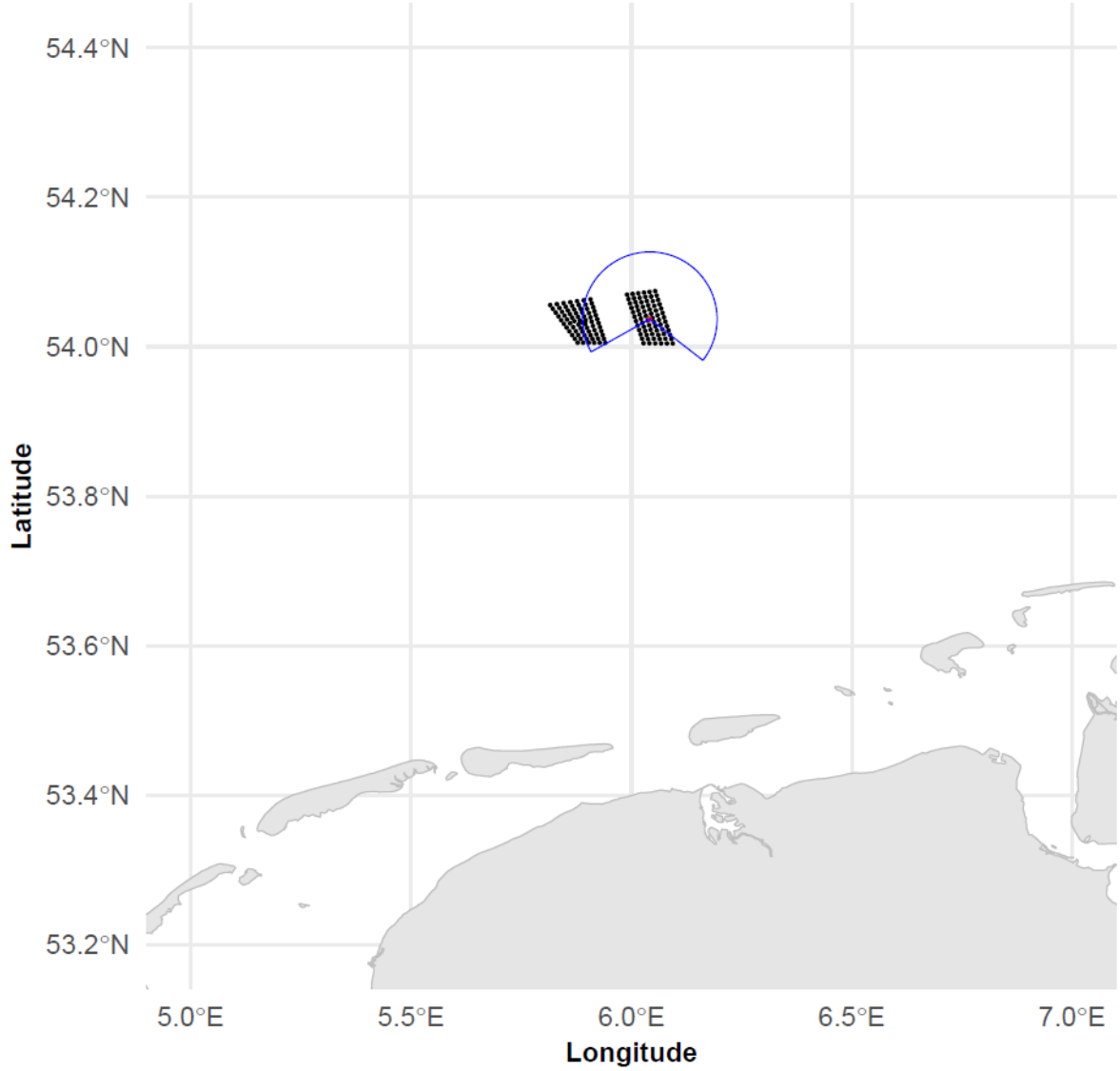


**Figure 1**. Overview of the study area. Black dots show the turbine locations of Gemini wind park. The red dot indicates the location of the Robin Radar 3D-Fix on the service platform of the east section of the wind farm (Buitengaats). The blue outline depicts the radar coverage as determined by the theoretical maximum distance of the radar (10 km) minus the angle at which the radar is blocked by the service platform (127° - 240°).

The Environmental Impact Assessment for Gemini wind park concluded that, due to the proximity to several Natura 2000 sites, the project could only be realized if bird populations of these areas would not be affected (Burggraaf-van den Berg et al. 2012). Additionally, birds migrating over the North Sea could be affected by the wind farm as well. The number of birds in the nearby area during breeding, staging, and migration is largely unknown due to the limited capacity to quantify birds offshore. The report estimated there would be no severe risk for birds but highlighted the importance of ongoing

monitoring. Several monitoring schemes were suggested, including ship surveys, GPS tagging of nearby breeding birds, and radar monitoring of birds within and near the wind farm. Additionally, to reduce the risk to migrating birds, the report suggested shut down during nights of predicted high intensity migration, but this was not required as the risk of collision was assessed to be low.

In addition to the EIA report, an Appropriate Assessment report indicated that northern gannets *Morus bassanus*, northern fulmar *Fulmaris glacialis*, and lesser black-backed gulls *Larus fuscus* from nearby Natura 2000 sites could be encountering the wind park based on their average foraging range and previous observations (Jonker et al. 2012). The additional mortality expected due to collision for these species, assuming a homogeneous distribution throughout the area, was between 0.64 and 1.71% for the colonies of lesser black-back gulls, 0.51% for the nearby northern gannet population, and 0.11% for the nearby northern fulmar population. Habitat loss was not assumed to be a concern for these species due to the small wind farm area relative to their foraging range. Additionally, the repost estimated 46 bird species were likely to cross the Southern North Sea during their migration, but due to the relatively small area of the wind park relative to the length of their migration route these species were not deemed to be affected during migration, with the highest additional mortality reported for the northern fulmar at 0.04%.

As part of Gemini's environmental monitoring program, the distribution of bird species in and around the wind farm area was surveyed on a monthly basis for one year, before construction of the wind farm commenced (van Bemmelen et al. 2015). The study confirmed that likely only low numbers of breeding birds from nearby Natura 2000 sites visited the area, including northern gannet, black-legged kittiwake *Rissa tridactyla*, common guillemot *Uria aalge*, and lesser black-backed gull. Several migrating species were observed, including divers, northern gannets, common scoters *Melanitta nigra*, little gulls *Hydrocoloeus minutus*, and terns, but the effect of the wind farm on these populations would be limited. The largest predicted impact was for wintering birds on the German bight, who would be pushed out of the area. Specifically, common guillemots might be affected as they are most numerous and tend to avoid the wind farm (Dierschke et al. 2016). A point of note is the limited study period of one year, as between-years variation is likely to occur and has yet to be examined.

Two projects in collaboration with the University of Amsterdam were funded to support additional monitoring in relation to Gemini wind park. The project "Offshore space use of Lesser Black-backed Gulls (Larus fuscus) from the Schiermonnikoog breeding population" (GEM-40-107) aimed to study the behaviour of lesser black-backed gulls of the Schiermonnikoog breeding population in relation to the environment and Gemini wind park. The most important results of that project are summarized (Sage and Shamoun-Baranes 2022) and include the PhD thesis of Dr. Elspeth Sage (Sage 2022). The project "Spatial and temporal dynamics of bird movement over the North Sea" (GEM-03-266) is the focus of the current report and describes the outcomes of the bird radar monitoring at Gemini wind park. The project was divided into two sub-projects (SP): the aim of SP1 was to develop an e-ecology infrastructure to store, manage, and explore dedicated bird radar data from Gemini wind park, the aim of SP2 was to quantify bird migration and bird densities at sea, especially at rotor height, in relation to environmental variables. The project ran parallel with the NWO-TTW project "Interactions between birds and offshore wind farms: drivers, consequences and tools for mitigation" (project nr. 17083) with a significant financial contribution from Gemini wind park and Rijkswaterstaat. This document provides the executive summary of the GEM-03-266 project. More detailed descriptions can be found in related scientific publications (Bradarić et al. 2020; Manola et al. 2020; van Erp et al. 2021, 2023, 2024) and a PhD thesis (van Erp to be submitted) resulting in part from this project and the NWO-TTW project.

## 1.2 Aims of this report

The primary aim of this report is to provide an overview of the results of SP1 (Chapter 2-3) and SP2 (Chapter 4-5). Additionally, we summarize the radar validations performed by Waardenburg Ecology (Chapter 6) and our main findings (Chapter 7) and provide a list of publications (Chapter 8).

- In Chapter 2 (SP1), we present an overview of the radar system, the e-infrastructure in place to process the radar data, and the parties involved for maintaining different sections of the monitoring infrastructure.
- In Chapter 3 (SP1), we present the data output of the radar system focusing on the most valuable data tables for bird monitoring. We also describe how to access these data and the available post-processing to increase the reliability of the data.
- In Chapter 4 (SP2), we explore the observed patterns of bird flight in and near Gemini wind farm on several temporal scales. We show how daily and nightly abundance fluctuates throughout the years, as well as daily flight patterns in winter, spring, summer, and fall.
- In Chapter 5 (SP2), we focus on spring and autumn migration and present the mean traffic rates and altitude distribution of bird flight during high-intensity migration nights in both seasons.
- In Chapter 6, we summarize the outcomes of the radar validation carried out by Waardenburg Ecology, which is presented in a separate report (Leemans and Bravo Rebolledo 2023), entitled: “Bird radar observations in offshore wind farm Gemini”.
- In Chapter 7, we present a summary of the findings in this report and provide an overview of related research that uses data or themes arising from this project.
- In Chapter 8, we present a list of scientific publications that resulted from this project.

# 2. Monitoring infrastructure

## 2.1 Radar monitoring

To remotely monitor bird flight in and around Gemini wind park, a Robin Radar 3D-Fix was installed on the northern corner of the service platform of Buitengaats (6.0417°N, 54.0370°E). The Robin Radar 3D-Fix was chosen to match infrastructure rolled out by Rijkswaterstaat in other wind parks at the time and to facilitate comparative analysis of bird movements across the North Sea. The Robin Radar 3D-Fix is a dedicated bird radar system consisting of a vertically rotating X-band antenna (25 kW, Furuno Marine, 43 m above lowest astronomical tide) and horizontally rotating S-band antenna (60 kW, Furuno Marine, 34 m above lowest astronomical tide), both rotating at 0.83 rotations per second (Fig. 2). The horizontal antenna has a theoretical detection range of 10000 m (10 km) for birds of 0.5 kg (1 standard avian target, or SAT) and scans the area between 240° and 127° (Fig. 2B). The vertical antenna has a theoretical detection range of 6000 m (6 km) for birds of 1 SAT and scans a vertical plane between 60° and 240° with a 20° width (Fig. 2B).

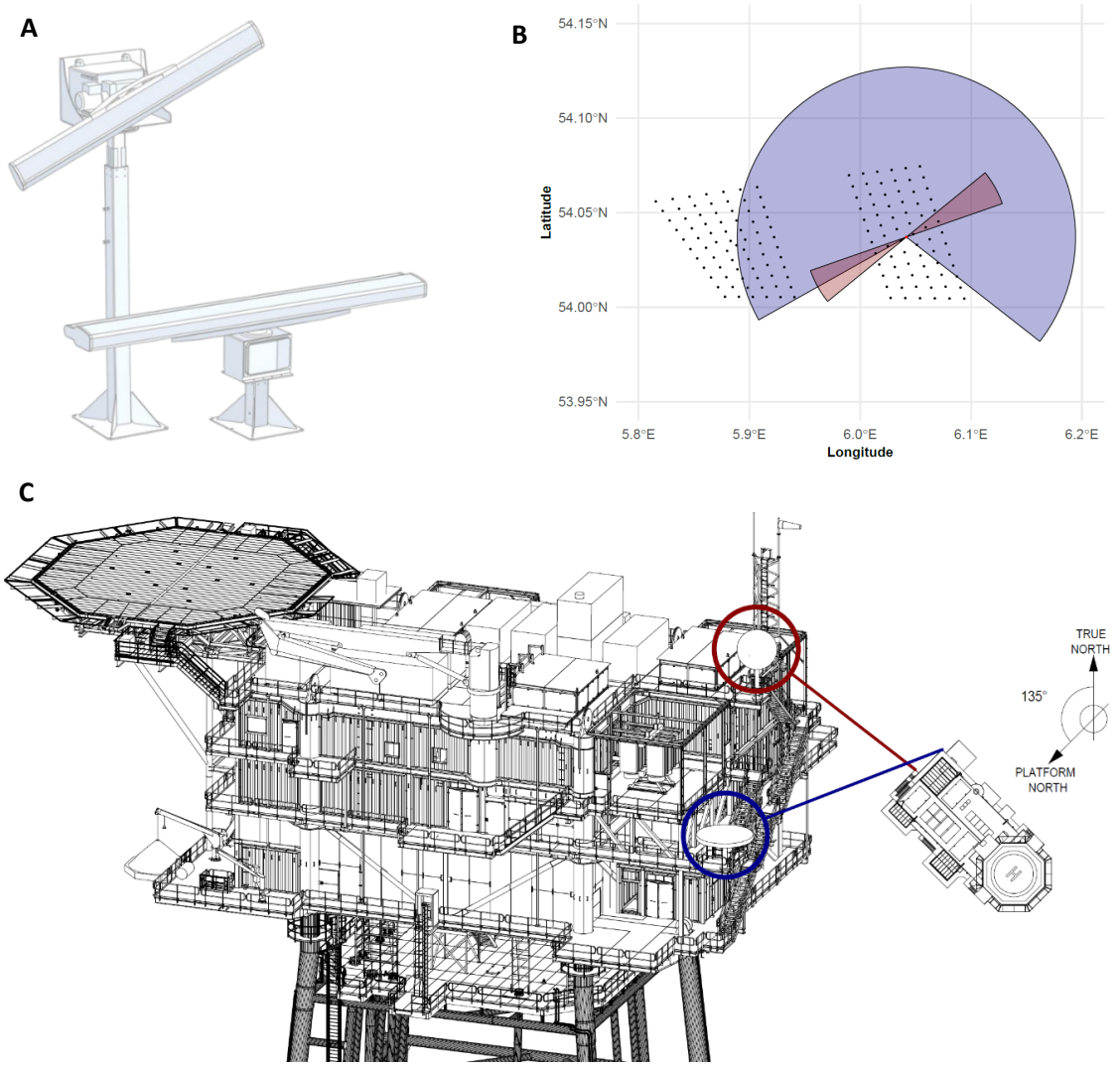


**Figure 2**. A: Vertical (top) and horizontal (bottom) antennas of the Robin Radar 3D-Fix system. B: Overview of Gemini wind park and the area covered by the radar antennas. Turbines are depicted as black dots. The horizontal antenna covers an area with 10000 m radius and is blocked by the service platform between 127° and 240° (blue). The vertical antenna scans a vertical plane between 60° and 240° with a 20° width (red). C: Location of the horizontal antenna (34 m above lowest astronomic tide, blue) and the vertical antenna (43 m above lowest astronomic tide, red) on the service platform.

The radar scans both planes simultaneously to detect targets by measuring the reflection of objects in relation to the background. Once a target has been detected, it is tracked by a tracking algorithm, and the reflective properties of the target as well as its derived airspeed (for targets observed by the horizontal antenna) are used to classify the target as a bird or non-bird. Birds are further classified as either small, medium, or large bird based on their reflective size, or as flock if the reflection has the property "IN_BLOB_FORMATION", which indicates multiple targets fly close together to create a single larger reflection. Consult the radar documentation for a complete overview of target classification. The reflective size of a bird depends on many factors, including their distance from the radar and which side of the bird reflects the radar beam. Additionally, there is no way to know the number of birds making up a flock. Therefore, in this report we do not distinguish between different bird classes and treat flocks as single bird observations. As the radar functions autonomously, the system can monitor birds year-round, unless it is turned off during maintenance or breaks.

## 2.2 Data flow & responsible parties

Tracking data and supporting information is stored locally at the radar for one month, after which it is automatically removed to free up space for new observations. Data is automatically retrieved by a data scraper that pushes the data to a centralized PostreSQL database hosted by SURF (Fig. 3). The Gemini wind park database is one component of the e-science infrastructure for bird movement monitoring and modelling developed by the University of Amsterdam (De Groeve 2023; Qi and Shamoun-Baranes 2024). The data is accessible by users with an account and the right permissions. This project contributed to the further development and sustainability of the e-science infrastructure, designed for long term collaborative research on avian movement. The infrastructure includes data from other mobile bird radars (e.g., from Rijkswaterstaat, the Royal Netherlands Air Force, UvA) and the UvA Bird Tracking System (www.uva-bits.nl), figure 3 provides an overview of the e-science infrastructure components directly relevant for this project.

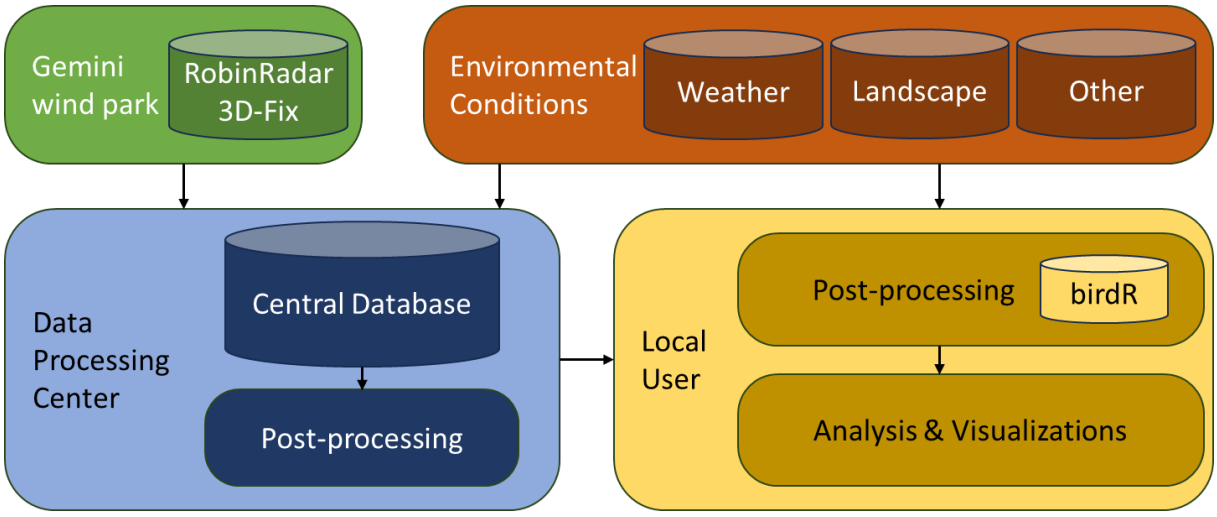


**Figure 3**. Schematic diagram of e-science infrastructure for monitoring and modelling bird movements with bird radar. The Robin Radar 3D-Fix tracking data is scraped to a central database for storage. Post-processing can be done in the data processing center, or by local users using tools such as birdR, or both. Some environmental conditions are stored centrally for general use and post-processing, while other conditions will be acquired by users. Analysis and visualizations are generally made locally as these are often project dependent.

Due to the complexity of the e-science infrastructure and parties involved, responsibilities for different parts lie with different organizations.

Robin Radar

- Hardware and software maintenance of the Robin Radar 3D-Fix, further specified in their contract with Gemini.

Gemini

- Owner of the radar system and radar data.
- Provision of power and data connectivity with the radar system.
- Providing access to the service platform for on-site maintenance.

University of Amsterdam

- Establishment of the radar database hosted at SURFsara and coordination of communication between Gemini and SURFsara.
- Definition of user requirements for SURFsara.
- Data quality monitoring.
- Tools for data exploration and post-processing.
- Using the data to study bird flight in relation to their environment and the wind park (see Section 1.2).

SURFsara

- Maintenance and service of the radar data database server.
- Security of the data connection between the radar system and the database
- Facilitation of database connections.
- Setting up “heart beats”: alarms which notify users when the data flow is interrupted.

# 3. Radar data

## 3.1 Data structure

The Gemini radar database has several schemas which host the radar data. The data coming in from the 3D-Fix radar system is hosted in the *public* schema and its 42 data tables. Although most of these inform on some aspect of the radar system, not all of these are important for bird monitoring. The tables that are most important for bird monitoring are listed below. Consult the database manual provided by Robin Radar for a more detailed explanation of each table.

### Classification

The *classification* table contains information on the classifications the radar system assigns to the radar tracks. Most importantly, the *id* column holds the identifier that is used in the track table (see below), and the *archetype* and *classification* column note whether the target is a bird and what class (small, medium, large, or flock) respectively. Note that due to an error, the rows are duplicated for this table in the Gemini radar database, meaning each class has a double entry and two ids (e.g., small bird targets have id's 14 and 15). It is therefore recommended to query bird tracks based on *archetype* or *classification*, rather than *id*.

### Image & Ip_metainfo

The term "image" relates to a single radar scan of the area. The *image* table contains information about each radar image acquired by the system. Most importantly, it contains the timestamp of each image, which can be related to the *ip_metainfo* table. The *ip_metainfo* table mainly contains summary information on the masking applied to each image to remove unwanted reflections from features that interfere with identification of bird targets, such as waves and rain.

### Observation

The *observation* table holds all validation measurements performed by Waardenburg Ecology, including the position, time, observed species, and some additional comments made in the field.

### Radar & Radartype

The *radar* and *radartype* table both hold information on the antennas of the radar system. *Radar* holds the name, position, and installment time of the antennas that have been mounted to the radar system throughout operation. *Radartype* holds information on the antenna model.

### Systemstatelog

The *systemstatelog* tracks the status of several hardware and software components of the radar system. The table can be used to troubleshoot problems with the radar and verify radar functioning during analysis.

### Track

The *track* table contains the tracks measured by the radar. The most important columns are the *timestamp_start* and *timestamp_end* (which mark when the track occurred), *trajectory*, and *trajectory_time,* which notes the time passed since the start of the track per trajectory point. The table holds many other informative columns describing aspects of the track, most importantly *classification_id* which shows whether the target is a bird or some other feature, *track_type* which notes which radar antenna measured the target, and *trajectory_radarid* which notes which point in the trajectory was measured by what antenna.

### Trackestimate

Now obsolete (since 2021-07-20 06:41), the table is maintained, as it still holds valuable information for the tracks measured before this date. The *trackestimate* table holds information on the individual points of each track, which can be identified by the *track_id* number. Most importantly, the table was used to obtain information on which antenna (*radar_id*) captured which track point and the timestamp per plot (*timestamp*), which are now reported in the *trajectory_radarid* and *trajectory_time* columns in the *track* table.

## 3.2 Accessibility

Data is stored on and accessible from the robin.e-ecology server hosted and maintained by SURFsara and administrated by the University of Amsterdam. Access is granted through a secure connection with account and password, which can be requested via J Shamoun-Baranes.

## 3.3 Post-processing

As described in section 2.2, the radar system classifies each observed tracks into a bird or non-bird class based on several track properties: reflective size and airspeed based on local wind measurements. This classification provides an initial separation of bird targets from other objects that reflect the radar, such as vessels, structures, and landscape features. However, due to the lack of available information and limited available processing time, the data can still contain tracks that are wrongly classified as birds (false positives). Additionally, the radar system can temporarily ignore areas around the radar for bird tracking if the amount of background noise is too high, such as during high sea states and rain. These periods could then be wrongly interpreted as moments no birds were flying near the radar (false negatives) and should therefore also be identified.

To post-process tracking data from the 3D-Fix, a post-processing framework was developed that provides additional filtering to increase the reliability of the data as well as to identify gaps in time and space where accurate bird tracking is problematic (Fig. 4). Below we describe the post-processing steps taken for the data presented in this report (R-scripts provided in Appendix 2). We use all horizontal and mixed radar tracks classified as birds between 1 Januari 2020 and 31 December 2022 as initial data input. A more detailed overview of this framework is provided in van Erp et al. (2024), available in Appendix 3) and the accompanying R-package for post-processing horizontal bird radar data (De Groeve and van Erp, 2023).

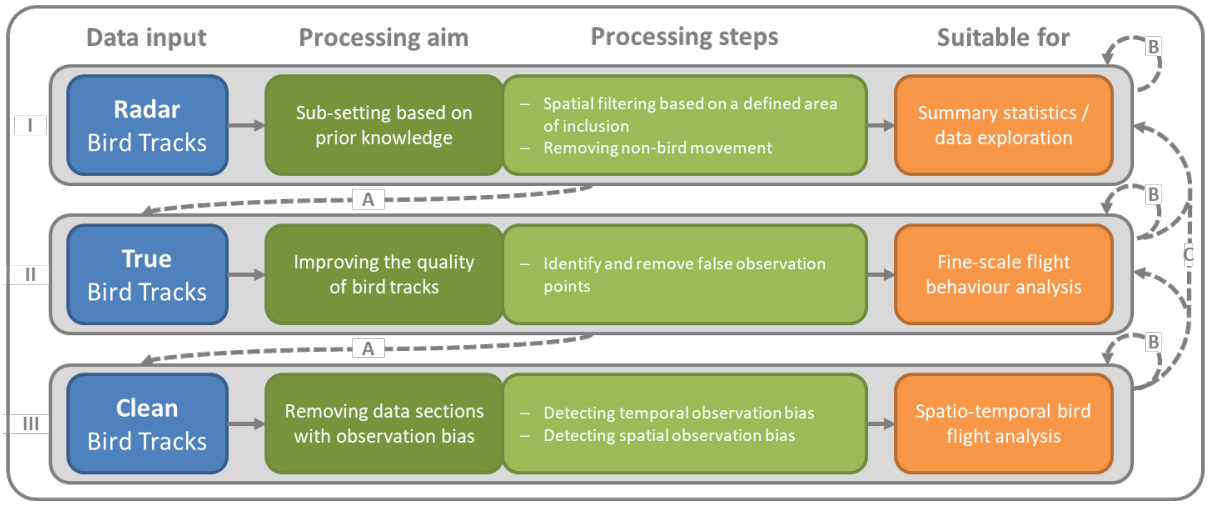


**Figure 4**. Overview of the radar data post-processing framework. The framework consists of three modules (I, II, and III), each working with a defined data input (blue boxes). 'Radar Bird Tracks' in Module I refers to all tracks classified as birds by the radar system. The subsequent data inputs ('True Bird Tracks' and 'Clean Bird Tracks') are subsets. Each processing aim (dark green boxes) is realised by one or several processing steps (light green boxes). After a module is applied, the output is suitable for specific purposes (orange boxes). Solid arrows show the logical progress within each module. Dashed arrows indicate the sequence of module application based on data verification and newly gained knowledge. Modified from van Erp et al. (2024).

### 3.3.1 Module I: sub-setting based on prior knowledge

We first set a spatial filter that removed tracks outside the area we considered reliable for bird tracking (the area of inclusion), based on four factors. First, close to the radar the high power of the radar beam causes increased reflection from the sea surface which often cause waves to be classified as birds, even at low sea states. Therefore, a minimum distance from the radar was set at 1000 m. Second, at far distance from the radar thee change of observing small birds becomes low as the power of the beam decreases. Therefore, a maximum distance from the radar was set at 2500 m, based on the theoretical probability of detection of small bird targets (-25 $dBm^2$). Third, the service platform the radar system is installed on blocks observations between an angle of 127-240° North. All tracks recorded in this area would be erroneous tracks. Fourth, the wind turbines create strong reflections, which can both obscure the weaker reflections of nearby birds and cause false observations. Therefore, the area within 100 m around the turbines was removed, based on the diameter of the rotor (130 m) plus a buffer. The resulting area of inclusion (Fig. 5) was used to subset the data: any track which did not (partly) overlap with this area was removed from further analysis. Initially, there were 91056158 bird tracks as classified by the 3D-Fix. The spatial filter removed 79963236 tracks, or 87.8 % (Table 1).

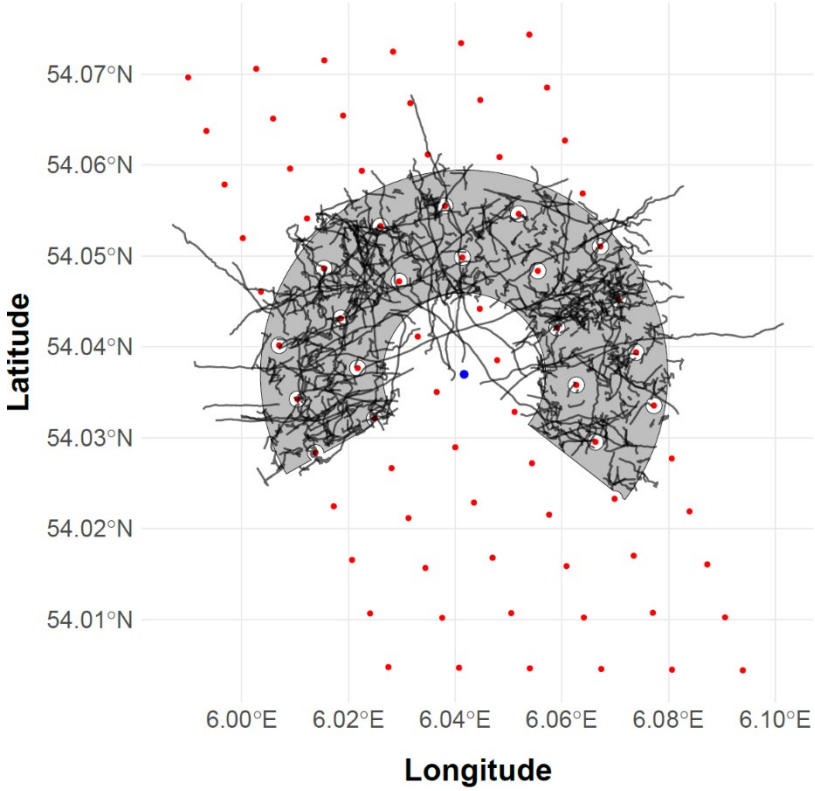


**Figure 5**. The area of inclusion (grey area) for the 3D-Fix radar system at Gemini wind park (blue dot). The area was set between 1000-2500 m distance from the radar, with the area blocked by the service platform (127-240° North) and within 100 m radius of the wind turbines (red dots) removed. Only tracks that (partly) overlapped with the area of inclusion (black lines) were retained for further analysis.

After spatial sub-setting, two filters that remove false positive bird tracks were applied. First, average airspeed was re-calculated with wind data from the ERA5 reanalysis from the European Centre for Medium-Range Weather Forecast according to Shamoun-Baranes et al. (2007). Based on measured airspeeds for seabirds (Spear and Ainley 1997), tracks with an average airspeed below 5 m $s^{-1}$ and above 30 m $s^{-1}$ were removed. Secondly, we found that often false positive bird tracks were classified

from tracks that exhibit specific “behaviour” in which the target moved back-and-forth in a very small area for extended periods of time. These types of tracks were identified by calculating the net displacement between the start divided by the duration of the track (displacement over time) and the area of the minimum rotated rectangle enclosing the track (minimum covered area). By visualizing the tracks falling in the lowest percentiles for both parameters, the tracks falling in the $5^{th}$ percentile of displacement over time (2.1 $ms^{-1}$) and the $15^{th}$ percentile of minimum covered area (0.5 $km^2$) were identified as false positives and removed. The two filters removed an additional 952312 false positive bird tracks (Table 1).

### 3.3.2 Module II: improving the quality of the bird tracks

Within each track, observation errors can occur due to anomalies or bugs in the radar tracking software. This can lead to isolated cases of extremely small time intervals between consecutive points and influence the classification of flight behaviour dependent on this information. Errors can be identified by determining the time interval between consecutive points in a track. Intervals that are considerably lower than the sampling frequency of the radar antenna likely indicate false observations. The threshold for false observations was set at 0.12 s, 10% of the observation interval for static objects (rotational speed of the 3D-Fix horizontal antenna = 1.2 s per rotation). 827463 out of 10140610 bird tracks (8.2 %) had one or multiple false observation points identified (Table 1). These tracks were corrected by removing the two points with this small time interval. After correcting these tracks, all their averaged track properties were re-calculated (track length, track duration, average ground speed, average airspeed).

### 3.3.3 Module III: Removing data sections with observation bias

As mentioned before, sections of the data could be less reliable to circumstances that cause increased background noise that obscures bird targets from the radar. These sections are unsuitable for temporal or spatial analysis of the data and should be identified and removed. Identification is split in two steps: first we identify periods of time in which the data is unreliable, second, we identify areas around the radar where the data is structurally unreliable.

The data can be temporally unreliable due to weather conditions affecting measured reflection, such as rainfall or high waves at sea, but periods where the system was offline due to malfunctioning or maintenance should also be considered. The 3D-Fix uses a set of spatial masks to prevent observations in areas with increased reflections (see also section 3.1). These variables are recorded any time that the radar is operational. Hence, time periods without mask entries denote moments that the radar was not operational. In total, the radar was offline for 3232 hours (Table 2), with a high proportion occurring in winter (see also Table 3). “Land mask” was used to establish whether the radar was masking due to high sea state, which is the most important factor. The tracking data was coerced to a temporal dataset; for each hour (except the hours the radar was offline) the number of clean bird tracks was counted, and the average hourly land mask intensity was calculated. The relation between hourly bird count and masking intensity was modelled by a generalized additive model (formula = hourly bird count ~ masking intensity) and visualised over the data together with the first derivative (Fig. 6). We calculated the landmask value where the $1^{st}$ derivative was at its minimum to find the value where the decrease was largest and used this as the threshold for data exclusion (landmask = 0.261). We considered the hours where this landmark threshold was exceeded to be unreliable, and these hours were therefore removed from the final dataset (13999 out of 23072 observation hours. A total of 476144 bird tracks occurred completely within these hours and were removed (Table 1).

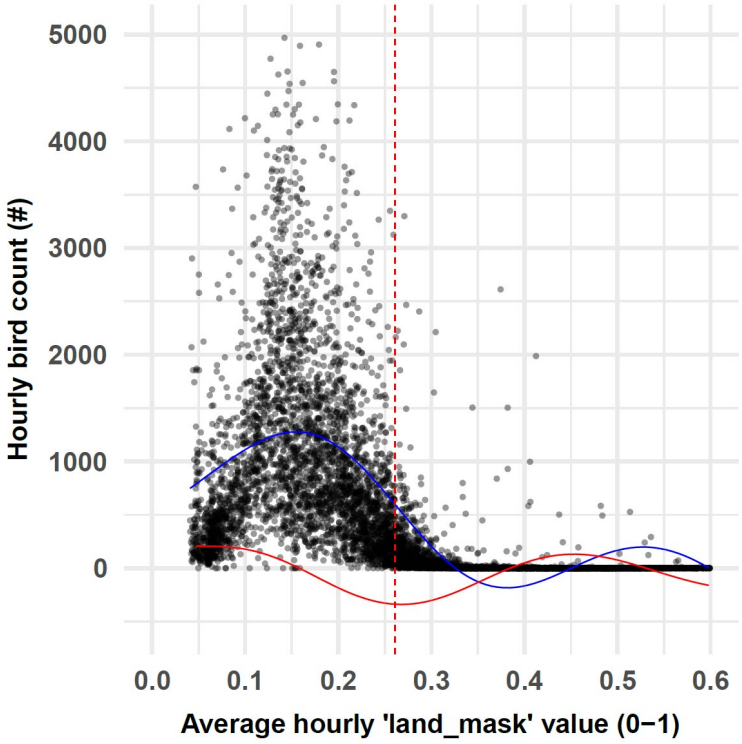


**Figure 6**. A scatter plot of hourly clean bird count against average hourly masking intensity shows declining bird counts with increasing masking intensity, which indicates a high proportion of false negative observations. This relation is estimated by a GAM (blue line). The 1st derivative of the trend line (red line) is used to set the threshold when the bias is considered too large (minimum of 1st derivative at 0.261, red dashed line).

Finally, although we applied a spatial filter in section 3.3.1 by setting the area of inclusion, there might be regions within this area where radar observations are obstructed that we did not anticipate, resulting in false negative observations. To identify these areas, a spatial raster of 100x100 m cells was created for the area of inclusion and the number of birds occurring per cell was counted (Fig. 7A). If movement through the area is homogenous, the number observations should be consistent throughout the area, and any cell with much higher or lower bird counts than its neighbours can indicate observations in that area are problematic. The relationship between the number of birds per cell and distance from the radar was estimated by fitting a generalized additive model to the data (formula = bird count per cell ~ distance from the radar), which was visualised on top of a scatter plot of bird count against distance from radar to see if observation bias occurred (Fig. 7B). Due to the ring of turbines at near-equal distance from the radar, lower number of birds were observed between 1100 - 1600 m. This affected the GAM estimation within this range and made it difficult to distinguish spatial bias. Therefore, we replaced the predicted bird counts of the GAM with a linear interpolation between the two maxima before and after this section (from 11180 birds at 1090 m to 8893 birds at 1604 m, Fig. 7C). Next, the predicted value minus 10 times the standard error was chosen as a threshold for identifying cells that have unreliably low bird counts, which marked 233 out of the 1115 cells (20.9%, Fig. 7D). These cells were not included in the final dataset and 296213 bird tracks which occurred entirely within the area of those cells were removed from the dataset (Table 1), tracks which intersected these cells were retained.

After application of all post-processing modules, 81687905 of the 91056158 bird tracks (89.7%) were removed, resulting in a dataset of 9368253 tracks for ecological analysis, observed over an area of 10.7 $km^2$ across 9054 hours between 01-01-2020 to 31-12-2022.

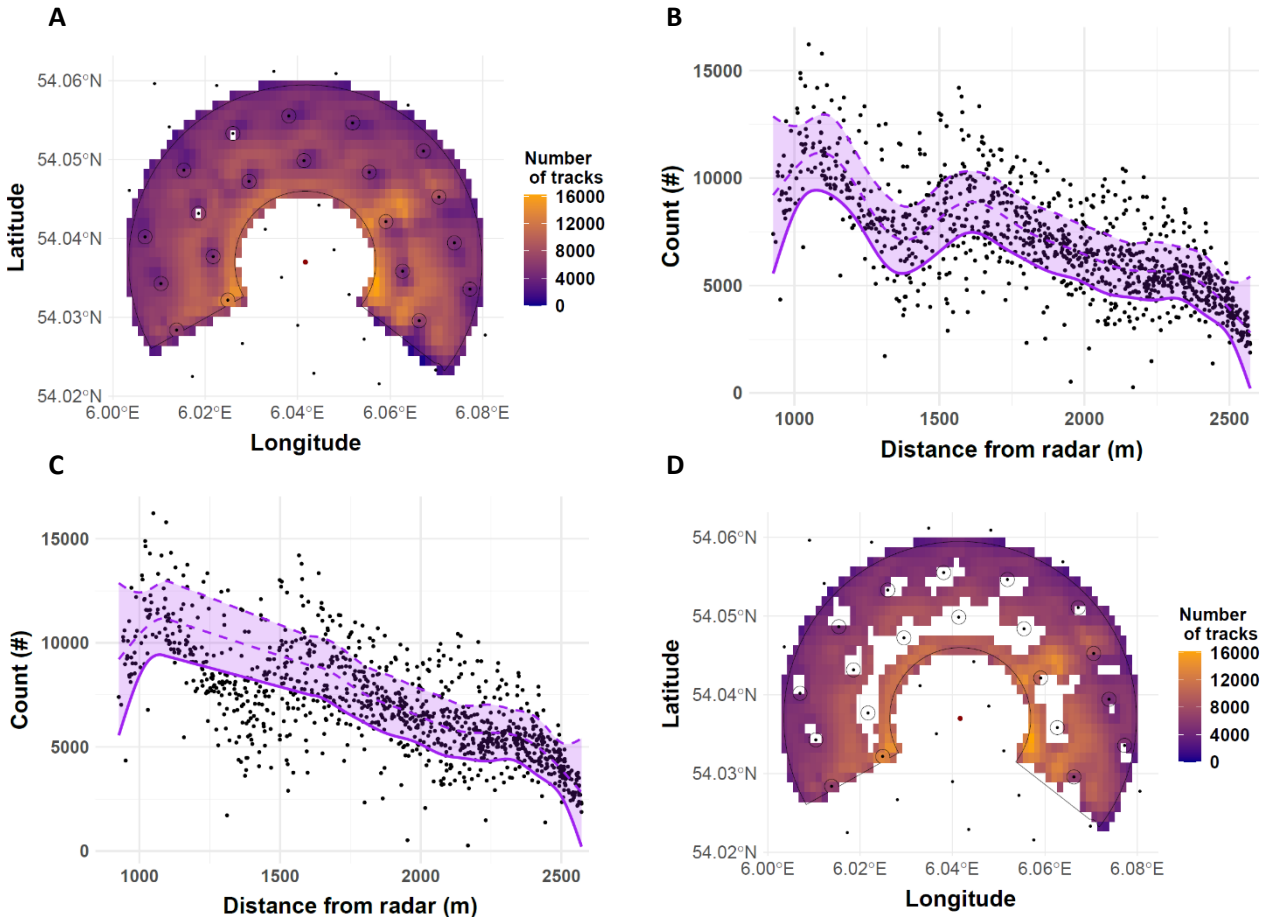


**Figure 7**. A: Spatial overview of number of birds per 100 x 100 m cell (blue to orange hue). The black outline depicts the AoI, black dots depict the individual turbines of the wind farm, the red dot indicates the location of the radar on the service platform. B: Scatter plot of bird count against distance from the radar for each cell. The trend is estimated with a GAM (middle dashed purple line). The purple area shows data lying within the predicted bird count ± 10 times the standard error of the prediction. A systemic reduction in bird counts is seen between 1100-1600 m from the radar which affects the GAM estimate. C: The same overview as (B), but now the bird count estimate between 1100-1600m is interpolated from the nearby maximum values. D: The same overview as A, but now the cells identified for having reduced bird counts (i.e., below the solid purple line in C) are removed. Removed cells were located mostly around the wind farm turbines and along the edges of the AoI. Note that the area near the turbines situated in the overlapping area between the horizontal and vertical antenna (see Fig. 2) is more likely to be reliable.

**Table 1**. Overview of the number of tracks that are removed and remaining (Modules I and III) or corrected (Module II) per post-processing step. The percentage of tracks removed or corrected is relative to the remaining tracks of the previous steps.

| (Module) Post-processing step | Number of tracks removed or corrected (#) | Number of tracks remaining (#) | Percentage of tracks removed or corrected (%) |
|---|---|---|---|
| (I) Spatial filtering based on a defined area of inclusion | 79963236 | 11092922 | 85.6 % |
| (I) Removing non-bird tracks | 952312 | 10140610 | 8.6 % |
| (II) Identify and remove false observation points within a track | 827463 | 10140610 | 8.2 % |
| (III) Identify and remove temporal observation bias | 476144 | 9664466 | 4.7 % |
| (III) Identify and remove spatial observation bias | 296213 | 9368253 | 3.1 % |

**Table 2.** Overview of the number of hours the horizontal radar was offline, the masking activity was too high, and the remaining hours available for analysis.

| | 2020 | | 2021 | | 2022 | |
|---|---|---|---|---|---|---|
| | Hours (#) | Percentage of total (%) | Hours (#) | Percentage of total (%) | Hours (#) | Percentage of total (%) |
| Total | 8784 | 100 | 8760 | 100 | 8760 | 100 |
| Offline | 1360 | 15.5 | 1373 | 15.7 | 499 | 5.7 |
| High masking activity (> 0.261) | 4856 | 55.3 | 4544 | 51.9 | 4608 | 52.6 |
| Remaining | 2558 | 29.1 | 2843 | 32.5 | 3653 | 41.7 |

# 4. Patterns of bird flight

Although bird flight offshore is highly variable, patterns that describe the general trend of flight and behaviour can be discerned. These patterns follow the seasonal behaviour that occurs on the Southern North Sea within most bird species in the region. In spring, birds migrate north and east towards their breeding ground at higher latitudes (Bradarić et al. 2020). In summer, the sea is dominated by breeding birds on the nearby coast that perform foraging trips at sea (van Erp et al. 2021). In autumn, most species migrate back south and west, crossing the sea to winter in England, southern Europe, and beyond (Shamoun-Baranes and van Gasteren 2011). In winter, winter guests stay on the North Sea individually or in large flocks (Fijn et al. 2018). The difference in motivation and species composition greatly contributes to the difference in flight patterns observed by the radar. Therefore, we present these patterns per season to create an annual overview (Chapter 4.1) and see how seasonal behaviour affects daily pattens of flight (Chapter 4.2).

## 4.1 Bird abundance throughout the seasons

The number of bird tracks, average ground speed, and average flight direction (i.e., the circular average) were calculated per hour over the complete study period (1 Januari 2020 and 31 December 2022). Hours in which the radar was offline or masking intensity was too high (see Chapter 3.3.3) were ignored. Data was split per season based on expected dominant bird behaviour: spring migration (February 15$^{th}$ to May 15$^{th}$), summer breeding (May 15$^{th}$ to August 15$^{th}$), autumn migration (August 15$^{th}$ to November 30$^{th}$), and wintering (November 30$^{th}$ to February 15$^{th}$). Hourly bird count was then modelled as function of week in the year and sun azimuth in a general additive model (GAM) per season as in van Erp et al. (2021) to reveal daily and seasonal patterns of abundance. Additionally, hourly bird counts during the day and at night as function of week in the year were modelled separately to see if seasonal flight was dominated by diurnal or nocturnal flight.

Most data were available in summer (3587 hours over three summers, Table 3), while observations were limited in winter (1074 hours over 3 winters). Bird abundance (the number of observed reliable bird tracks per hour over the total area) ranged from 0 to 21546 birds per hour (maximum on 2021-09-13 15:00:00 UTC) over the study period. On average, abundance was lowest in the breeding season during summer (May 15$^{th}$ to August 15$^{th}$; Fig. 8 and Table 3), and at night in winter (Fig. 10). Bird abundance varied more in spring and autumn (Fig. 8), especially at night (Fig. 10), throughout the season as well as within each week (as seen by the wide error margins of the prediction in Fig. 8 and 10). In spring, bird abundance peaked in March, whereas in autumn peak abundance occurred over a longer period, between September to November. In winter, bird abundance varied more during the day (Fig. 9) and was consistently low at night (Fig. 10).

**Table 3**. Overview of available data, observed bird abundance, and average flight properties per season.

| Season | Period | Hours of data (#) | Average abundance (# per hour) | Maximum abundance (# per hour) | Average ground speed [day/night] ($ms^{-1}$) | Average direction [day/night] (°) |
|---|---|---|---|---|---|---|
| Spring | 15-02 to 15-05 | 2211 | 993 | 14988 | 15.0 [14.5 / 15.7] | 114 [137 / 94] |
| Summer | 15-05 to 15-08 | 3587 | 779 | 6472 | 13.9 [13.8 / 14.8] | 166 [137 / 168] |
| Autumn | 15-08 to 01-12 | 2201 | 1480 | 21546 | 14.1 [13.7 / 14.6] | 197 [173 / 213] |
| Winter | 01-12 to 15-02 | 1074 | 1141 | 7720 | 14.7 [14.3 / 15.1] | 157 [158 / 155] |

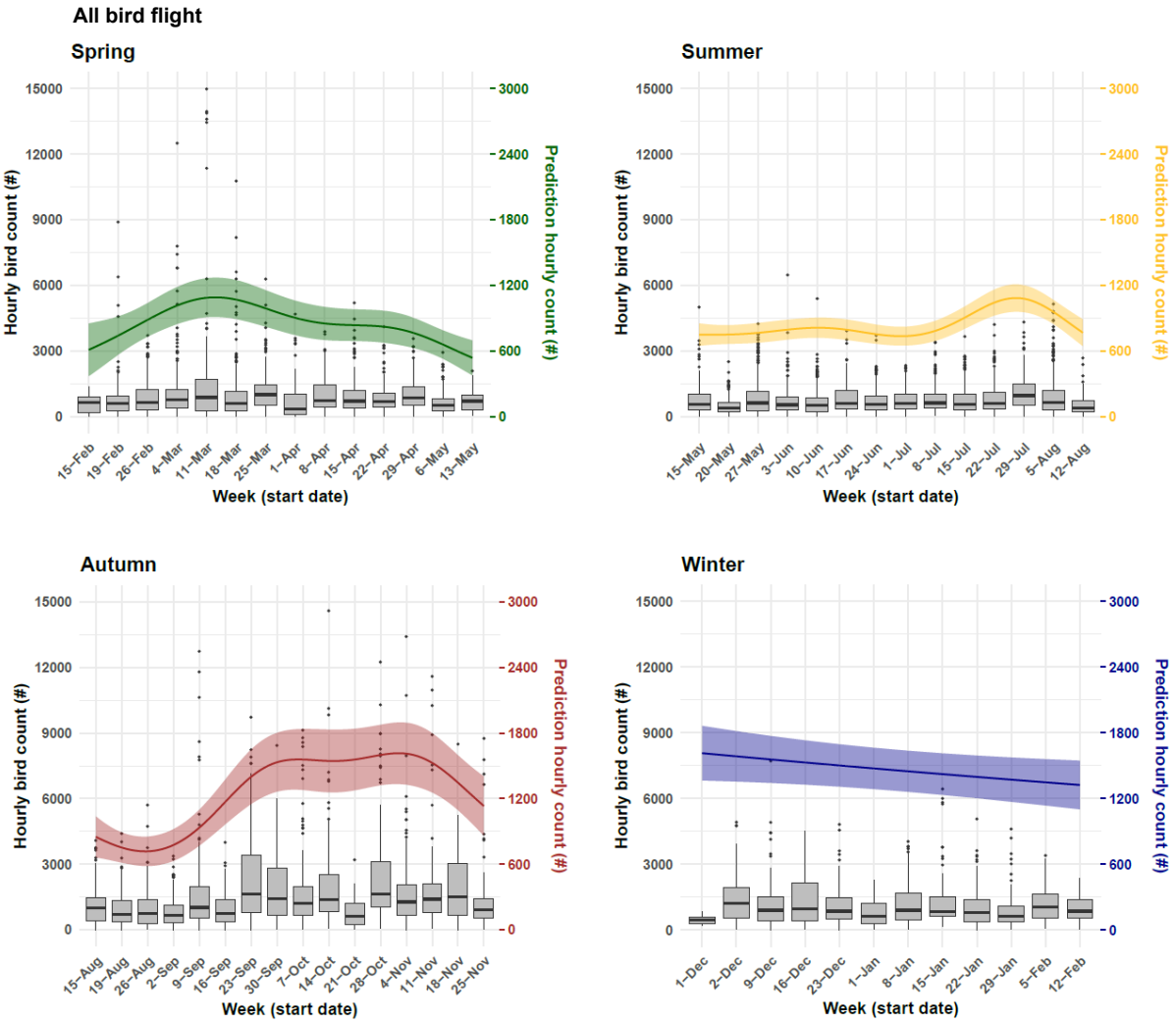


**Figure 8**. Hourly bird count per week (boxplots) and smoothed effect of week on hourly bird count (coloured line and ribbon) for observed bird flight in each season (spring: green, summer: yellow, autumn: brown, winter: blue). Left y-axes show observed hourly bird count, right axes show predicted bird count, x-axis shows the first day of each week of data.

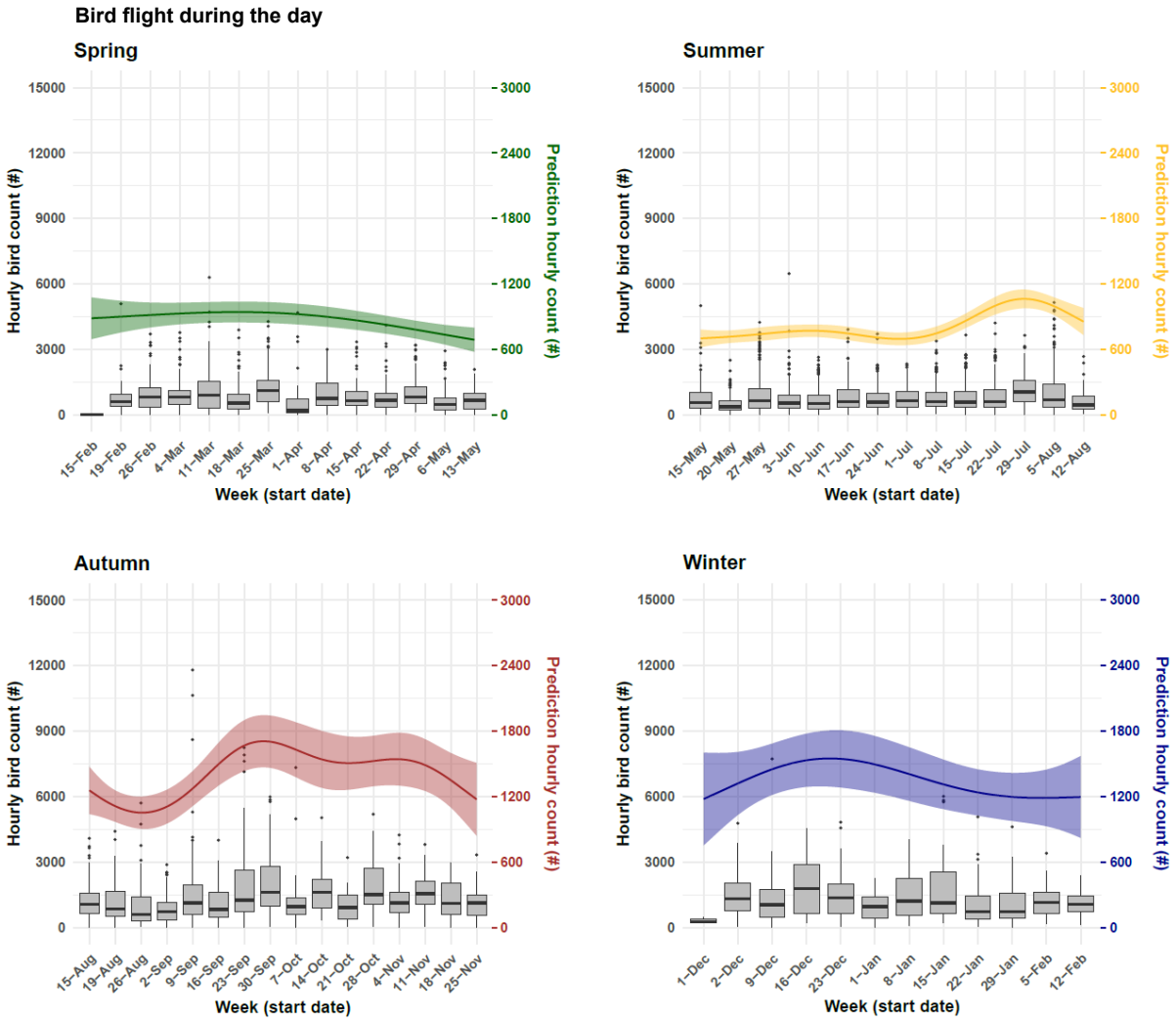


**Figure 9**. Hourly bird count per week (boxplots) and smoothed effect of week on hourly bird count (coloured line and ribbon) for observed bird flight during the day in each season (spring: green, summer: yellow, autumn: brown, winter: blue). Left y-axes show observed hourly bird count, right axes show predicted bird count, x-axis shows the first day of each week of data.

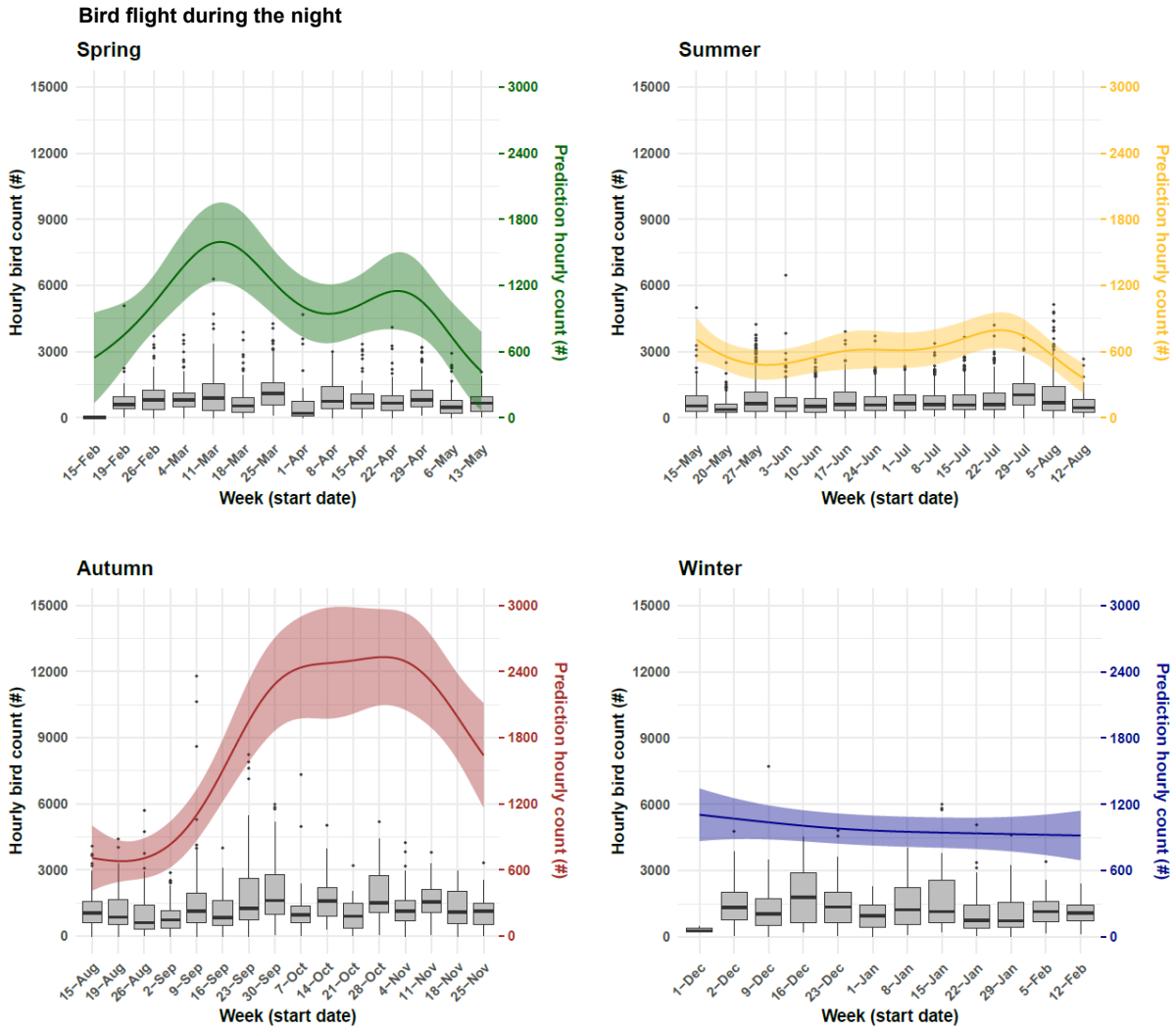


**Figure 10**. Hourly bird count per week (boxplots) and smoothed effect of week on hourly bird count (coloured line: mean and ribbon: 2*standard error) for observed bird flight during the night in each season (spring: green, summer: yellow, autumn: brown, winter: blue). Left y-axes show observed hourly bird count, right axes show predicted bird count, x-axis shows the first day of each week of data.

In order to investigate flight per seasons, we created density distributions of average ground speed per season for flight during the day and at night (Fig. 11). Average ground speed of observed birds ranged from 0.5 to 40.3 $ms^{-1}$, with most birds flying between 10 to 20 $ms^{-1}$. Ground speed differed little between seasons, although the appeared to be a slight difference in ground speeds observed in summer (13.9 $ms^{-1}$, Table 3) and autumn (14.1 $ms^{-1}$) and in spring (15.0 $ms^{-1}$) and winter (14.7 $ms^{-1}$), especially during the day (Fig. 11). Ground speeds were generally higher at nights compared to during the day throughout the year (difference of 0.8 – 1.2 $ms^{-1}$, Table 3).

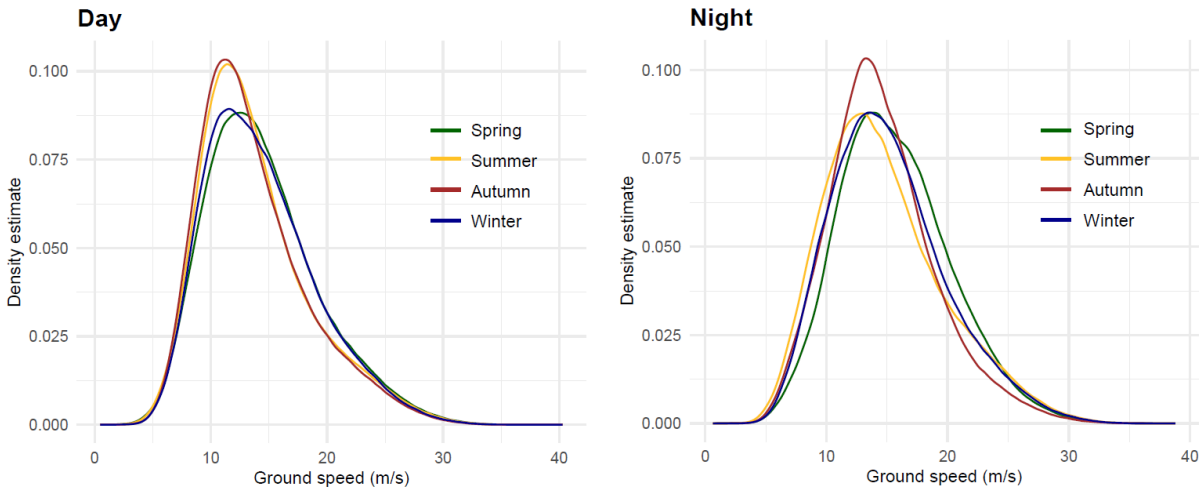


**Figure 11**. Density distribution of average ground speed in each season (spring: green, summer: yellow, autumn: brown, winter: blue) for day and night.

We show the distribution of measured flight directions through circular histograms (Fig. 12). South to south-east flight directions were dominant during diurnal flight, as well as at night during summer and winter (Fig. 12, Table 3). This flight direction is probably caused by bird flying towards the nearest coast (the Wadden Islands, Friesland, and Groningen) to the south-south-west. However, the lack of flight in the opposite direction is remarkable, as especially during the day and in the breeding season, we expect flight to be dominated by foraging birds that fly out to sea and return in a back-and-forth pattern (e.g., Fijn et al. 2017). Nocturnal flight in spring was mainly towards the east to north-east, while nocturnal flight in autumn was mostly in a west to south-west direction. These observed directions roughly follow the expected migratory axis observed in the North Sea off the western coast of the Netherlands (Bradarić et al. 2020). Intense migration in autumn with SE-SW track directions was also observed by military radar over sea, north of the Wadden Sea islands (Shamoun-Baranes and van Gasteren 2011).

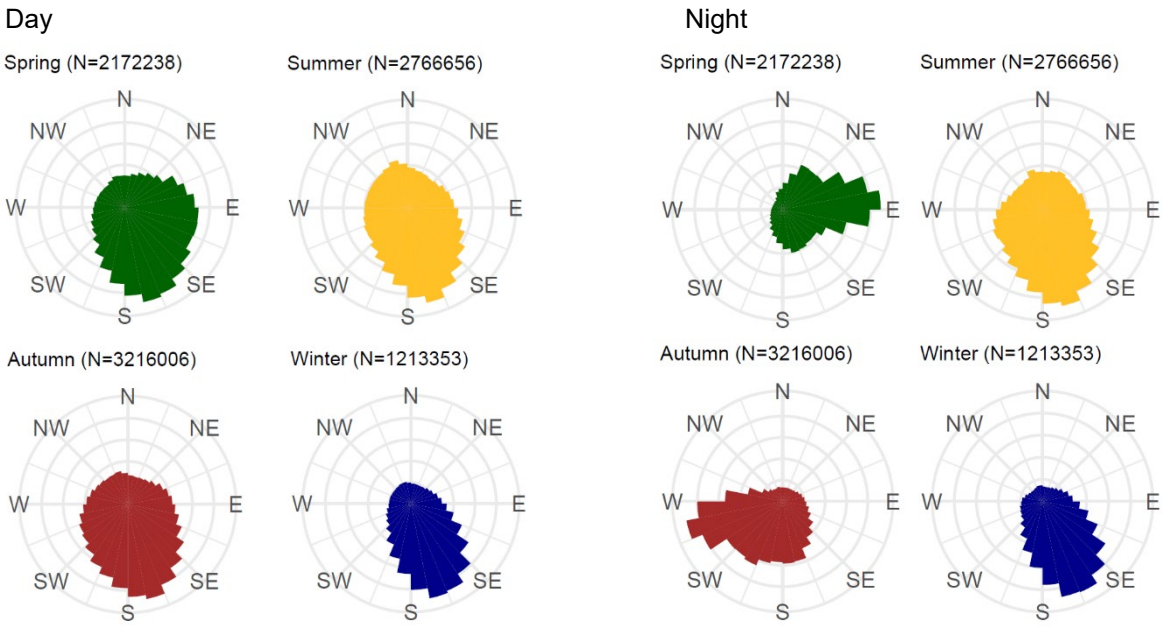


**Figure 12**. Circular histograms of flight directions in each season (spring: green, summer: yellow, autumn: brown, winter: blue) for day and night. The total number of tracks considered for each.

## 4.2 Daily patterns of bird flight throughout the seasons

The patterns of daily abundance (Fig. 13) show how differences in dominant bird behaviours drive the number of birds passing through Gemini wind park. In spring, we see that average bird abundance is highest late at night and early in morning (01:00 – 04:00 UTC). Based on the dominant flight direction (Fig. 12) and this late timing, this peak is likely caused by birds that left the United Kingdom and fly toward Denmark, rather than birds coming from Netherlands, as we would expect these birds to pass Gemini much earlier at night assuming they leave around sunset. In summer, bird abundance is following an expected pattern of higher bird numbers during the day, especially after sunrise (03:00 – 05:00 UTC), and low bird numbers at night. This pattern is similar to that found in order parts of the Dutch North Sea (van Erp et al. 2021). In autumn, bird abundance is high throughout the night, as Gemini wind park sees two peaks of abundance: one after sunset (21:00 – 23:00 UTC) and a second one during dawn (03:00 – 06:00 UTC). We expect these to be two waves of migrants: an initial wave from Denmark that have a shorter distance to cover before passing Gemini, and another wave from Norway and Sweden that pass the wind park in the early morning after a long flight (Shamoun-Baranes and van Gasteren 2011). Lastly, in winter we see a similar pattern as in summer, with higher activity during the day and lower activity at night. However, due to the limited availability of sunlight, the active period is much shorter (08:00 – 16:00 UTC). Additionally, there seems to be more variability in the numbers (seen by the wider model error margins in Fig. 13).

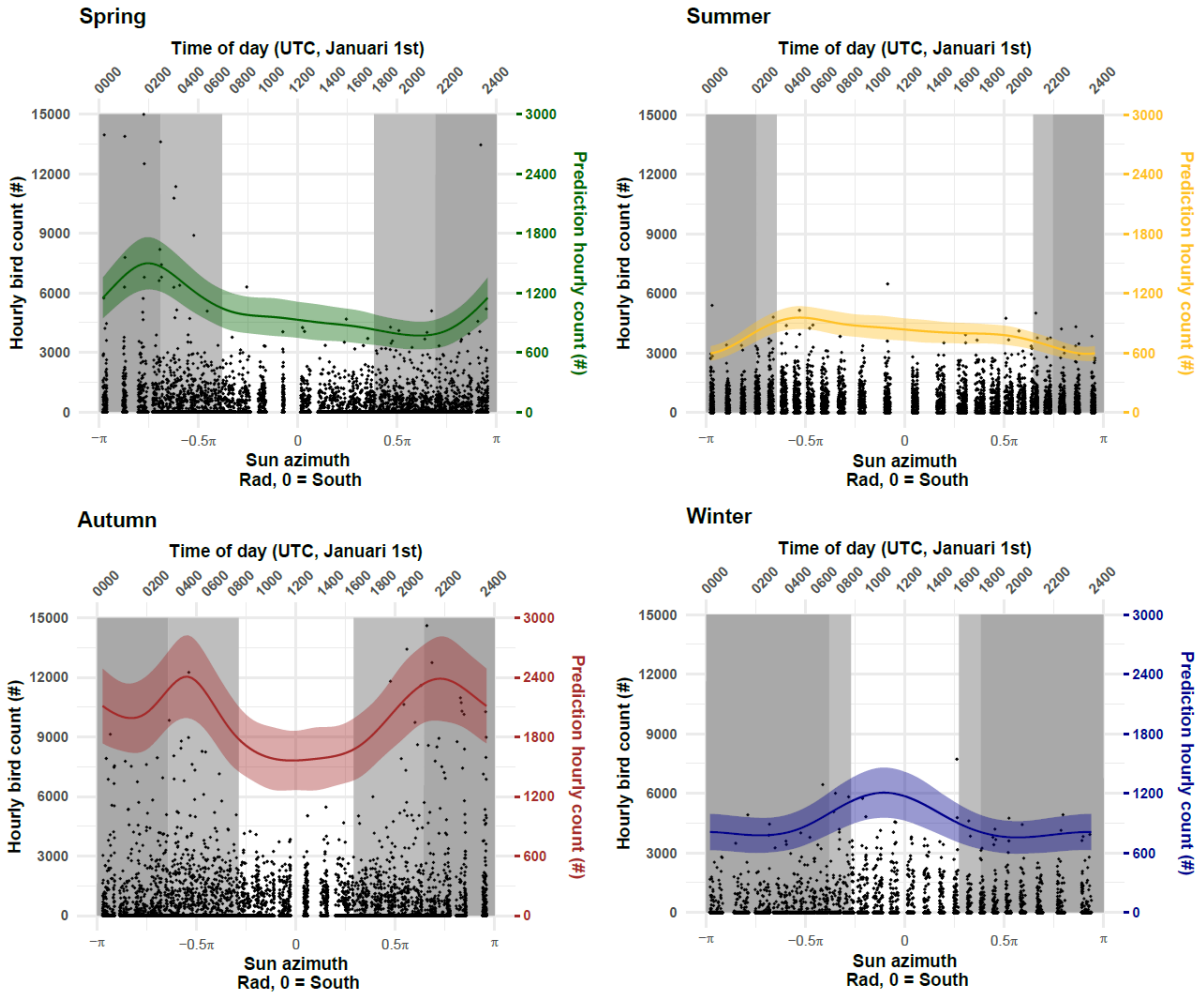


**Figure 13**. Hourly bird count throughout the day (black dots) and smoothed effect of sun azimuth as a proxy of time of day on hourly bird count (coloured line: mean and ribbon: 2*standard error) in each season (spring: green, summer: yellow, autumn: brown, winter: blue). Left y-axes show observed hourly bird count, right axes show predicted bird count, bottom x-axes show the sun azimuth, top x-axes show the approximate time (based on January 1st).

# 5. Migration in spring and autumn

For all nights in the spring and autumn season, the MTR (mean traffic rate) was calculated as outlined in Chapter 5 of Bradarić 2022:

$$MTR = \frac{t_p}{r \times a} \times gs$$

Where *MTR* is the number of birds per kilometer per hour (birds km$^{-1}$ h$^{-1}$), $t_p$ is the number of track points observed in a specific hour, *r* is the rotational speed of the radar (rotations per hour), *a* is the observed area (km$^2$, in this study the area of inclusion), and *gs* is the average groundspeed of all tracks in that hour. Only tracks with a straightness > 0.7 were used, as we assume migratory birds to have relatively straight flight paths. Hourly MTRs fluctuated from 0 to 925 birds km$^{-1}$ h$^{-1}$ (Fig. 14). Intense migration nights were selected based on an average nightly MTR higher than the average MTR across all hours between dusk and dawn (34 birds km$^{-1}$ h$^{-1}$). Across the three years we identified 34 nights of intense spring migration and 32 nights of intense autumn migration were identified between January 1$^{st}$ 2020 and December 31$^{st}$ 2022 (Fig. 14). For a full overview of hourly MTR over all nights, see the supplementary material (p. 32 – 36). The ten most intense migration nights were selected per season (spring and autumn) for further exploration (Table 4). In spring, migration tended to be less intense, although the 14$^{th}$ of March 2022 was an exception with an average MTR of 521 birds km$^{-1}$ h$^{-1}$ and a maximum MTR of 985 birds km$^{-1}$ h$^{-1}$. Average flight directions differed from 43° (north-east) to 108° (east). In autumn, higher average MTRs were recorded during the ten most intense nights, which agrees with the patterns shown in Chapter 4. Here as well, average flight directions differed between nights, from 179° (south) to 259° (west).

**Table 4**. Top ten highest intensity migration nights for spring and autumn migration (2020 – 2022). Nights were selected based on average MTR per night. Date is presented as yy-mm-dd. Direction represents the circular mean of track directions each night.

| Date | Average MTR (# km$^{-1}$ h$^{-1}$) | Max. MTR (# km$^{-1}$ h$^{-1}$) | Direction (°) | Date | Average MTR (# km$^{-1}$ h$^{-1}$) | Max. MTR (# km$^{-1}$ h$^{-1}$) | Direction (°) |
|---|---|---|---|---|---|---|---|
| 20-03-18 | 86 | 325 | 108 | 20-10-16 | 238 | 551 | 235 |
| 20-04-06 | 103 | 228 | 83 | 20-11-07 | 363 | 889 | 255 |
| 20-04-11 | 124 | 297 | 55 | 20-11-26 | 284 | 700 | 245 |
| 21-03-24 | 129 | 380 | 78 | 21-09-25 | 142 | 247 | 179 |
| 21-04-19 | 113 | 173 | 43 | 21-09-26 | 156 | 366 | 209 |
| 21-04-20 | 147 | 268 | 45 | 21-10-06 | 251 | 690 | 179 |
| 22-03-09 | 154 | 333 | 81 | 21-10-08 | 190 | 572 | 232 |
| 22-03-14 | 474 | 925 | 75 | 21-11-02 | 179 | 507 | 196 |
| 22-03-24 | 108 | 480 | 95 | 21-11-03 | 221 | 593 | 203 |
| 22-04-13 | 95 | 174 | 66 | 22-11-12 | 393 | 711 | 259 |

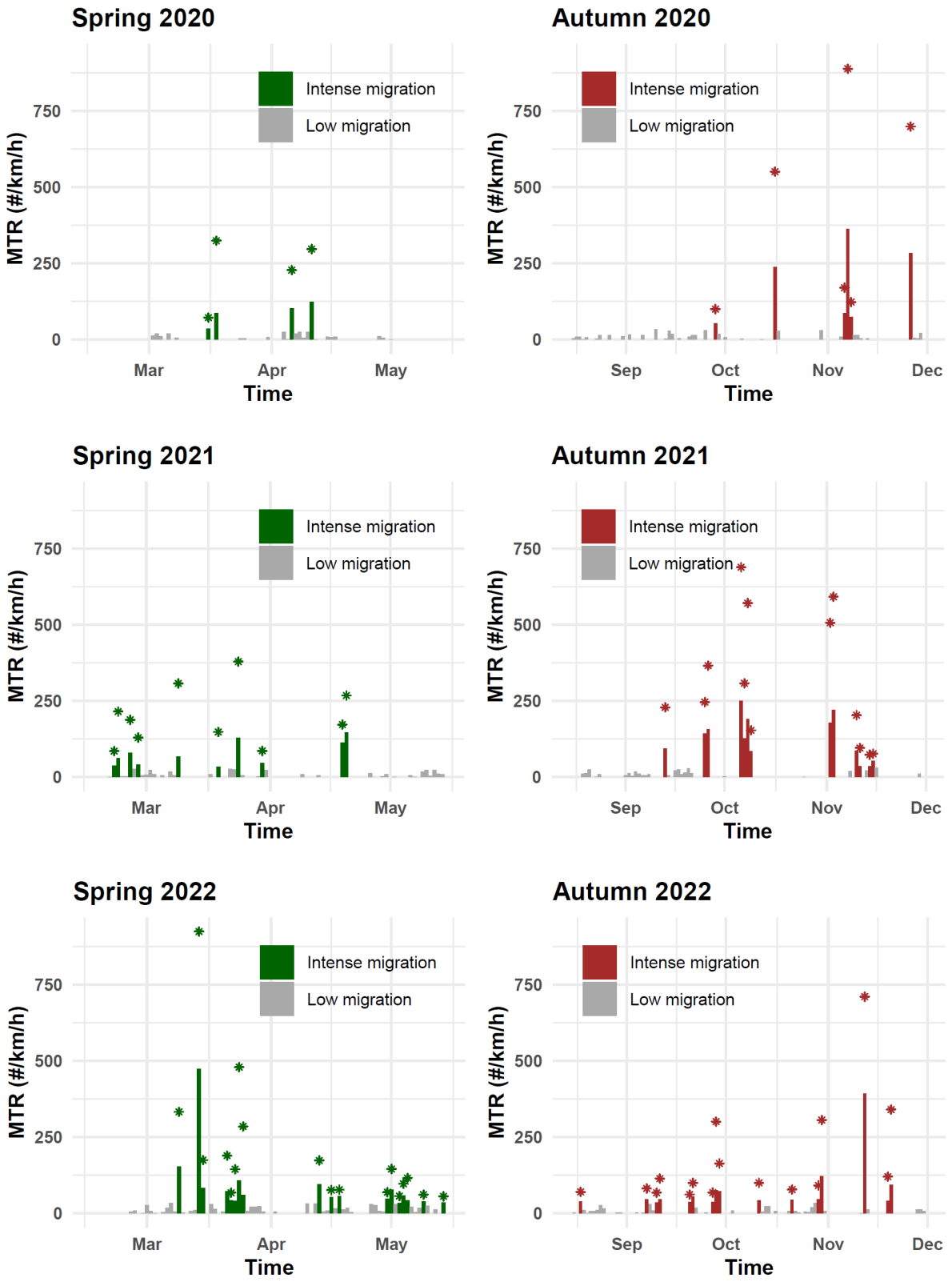


**Figure 14**. Overview of nightly mean traffic rates (MTR) for all nights in the spring (left) and autumn (right) seasons of 2020 to 2022. Nights in which intense migration occurred (nightly MTR > average MTR) are coloured (spring = green, autumn = brown), with the maximum hourly MTR on intense nights depicted with asterisks. Missing bars indicate days for which no data was available.

Data from the vertical radar was retrieved for all nights in the spring and autumn season. Due to the differences in antenna, these data were acquired and post-processed separately (Appendix 2). Only vertical tracks occurring between 500 – 1500 m from the radar and with an average altitude between 5 m and 1500 m were considered (Bradarić 2022). To explore bird flight altitudes during these nights, altitude density estimations were created per year for each season (Fig. 15). Most migration occurred within the rotor height of Gemini wind park, between 23.5-153.5 m, up to 84.3 % of observed flight (Spring 2021, Table 5).

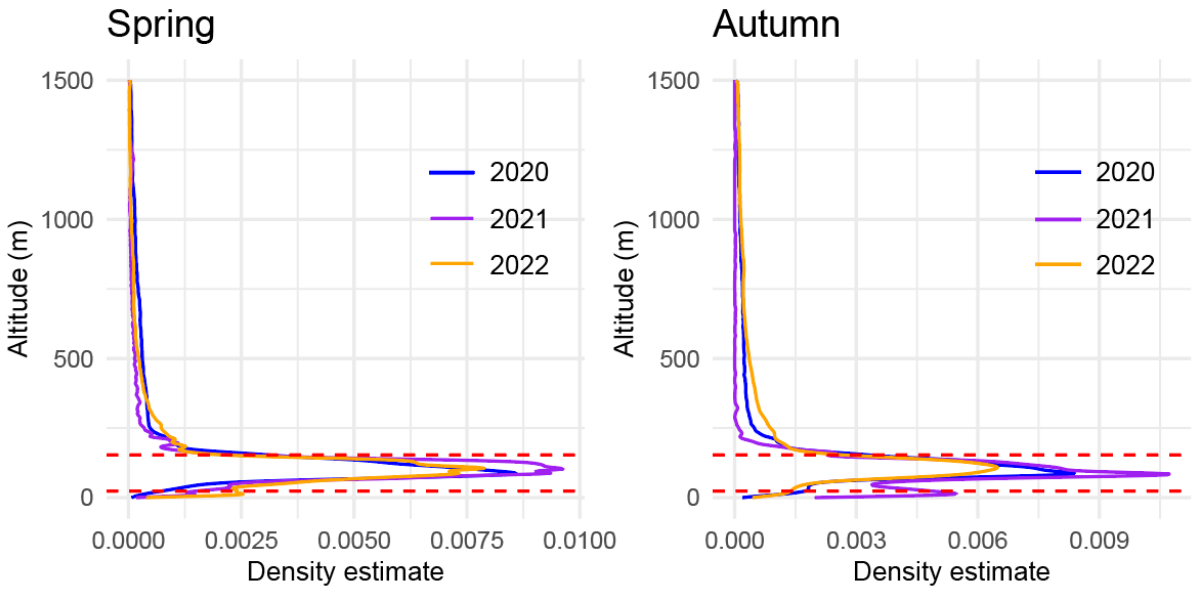


**Figure 15**. Density distribution of average flight altitude for birds observed by vertical radar during high intensity migration nights (as identified in horizontal radar). Data is split per season (spring = left and autumn = right) and per year (2020 = blue, 2021 = purple, 2022 = yellow). The red dotted lines indicate rotor height at Gemini wind park (23.5 to 153.5 m).

**Table 5**. Altitude metrics for birds observed by vertical radar during high intensity migration nights (as identified in horizontal radar) per season and year. Total metrics are calculated over the data of all years per season combined.

| | Median flight altitude (m) | Mean flight altitude (m) | Birds flying within rotor height (%) |
|---|---|---|---|
| Spring | | | |
| 2020 | 123 | 249 | 63.5 |
| 2021 | 110 | 167 | 78.0 |
| 2022 | 112 | 185 | 67.0 |
| Total | 115 | 207 | 66.5 |
| Autumn | | | |
| 2020 | 120 | 241 | 64.2 |
| 2021 | 88 | 94 | 79.1 |
| 2022 | 134 | 278 | 54.9 |
| Total | 131 | 269 | 57.1 |

# 6. Radar validation

On seven days in 2020 and 2021, validation measurements were carried out by Waardenburg Ecology to verify the accuracy of the radar measurements and provide visual validation for the radar tracks (Leemans and Bravo Rebolledo 2023, report added as Appendix 4). The most important outcomes are summarized here.

A three-step protocol was performed to:

1. Record absolute numbers of birds of all species throughout the day
2. Collect bird flight paths at different altitudes and distances from the radar
3. Determine the proportion of false positive and false negative radar observations.

The number of birds observed ranged from 0.1 to 0.6 birds per minute. On 5 out of 7 observation days average wave height was above 100 cm and the radar filtered the complete observation area, resulting in a false negative rate of 100 % on the horizontal radar. On both days with lower wave height, false negative rate was 0 %. Wave height was less of an issue for the vertical radar, but sample sizes were very low (11 observations over 7 days). Several radar tracks were annotated with species observations. Black-legged kittiwakes *Rissa tridactyla* and common gulls *Larus canus* made up most observations, others including great black-backed gull *Larus marinus*, herring gull *Larus argentatus*, lesser black-backed gull, great cormorant *Phalacrocorax carbo*, northern gannet, and sparrowhawk *Accipiter nisus* (Table 6).

**Table 6**. Number of true-positive validated radar tracks per observation day and observed species.

| | 07-07-20 | 08-09-20 | 19-05-21 | 18-08-21 | 14-09-21 | 17-11-21 | 14-12-21 | Total |
|---|---|---|---|---|---|---|---|---|
| Black-legged kittiwakes | | 2 | 2 | | | | 15 | 19 |
| Common gull | | | | | | | 18 | 18 |
| Lesser black-backed gull | | | 3 | | 1 | | | 4 |
| Greater black-backed gull | | | | | | | 1 | 1 |
| Herring gull | | | 1 | | | | | 1 |
| Gull sp. | | | 1 | | | | 1 | 2 |
| Northern gannet | | | 1 | | | | | 1 |
| Great cormorant | | | | | 2 | | | 2 |
| Sparrowhawk | | | 2 | | | | | 2 |
| Total | 0 | 2 | 10 | 0 | 3 | 0 | 35 | 50 |

During the observations days bird flight activity was generally low. Additionally, weather circumstances on most observation days were unfavourable for radar detection due to high waves and therefore strong filtering. Filtering is highest near the radar and as the observers were situated on the service platform close to the radar, the minimum distance at which the radar monitored birds was too far for visual observations. According to Robin Radar Systems, the first 600 m from the radar is suboptimal for bird observations, which was also confirmed by a high number of false negative observations of birds. Therefore, the report suggests performing validation measurements further away from the radar in subsequent studies. Due to the small sample size of vertical radar, no validation of that antenna could be performed.

# 7. Conclusions

In this report we provide an overview of the results of the project “Spatial and temporal dynamics of bird movement over the North Sea” (GEM-03-266). We looked at the established infrastructure and post-processing methods available for bird radar data and described the patterns of flight observed by the Robin Radar 3D-Fix installed at Gemini wind park in 2020 to 2022. Additionally, we summarized the validation measurements carried out by Waardenburg Ecology.

Bird flight at Gemini wind park follows a seasonal and daily pattern which is assumedly caused by shifts in species distribution and movement behaviour throughout the year. In the breeding season, from May 15$^{th}$ to August 15$^{th}$, most birds at sea are performing diurnal foraging trips (Shealer 2002). Due to the large distance between Gemini wind park and the nearest breeding colonies, the area sees relatively little activity in summer, as it lies at the edge of the foraging range of the most occurring seabird species, such as the lesser black-backed gull (Sage and Shamoun-Baranes 2022). In spring and autumn, nocturnal migration through the area creates hours with high bird traffic. These migratory movements are weather dependent as migrants select favourable weather conditions for their journeys (Shamoun-Baranes and van Gasteren 2011; Manola et al. 2020), which results in larger fluctuations in bird abundance within and between weeks, especially in autumn, when optimal conditions for migration occur less frequently. During these nights, migrants tended to follow an east-west axis of flight, along the coast of the Netherlands, although in autumn southward migration was also observed which, together with a second nocturnal peak in hourly counts, indicates an additional migratory wave from Norway (Shamoun-Baranes and van Gasteren 2011; Bradarić et al. 2020). In winter, activity is highest during the day, but fluctuates more than in summer, whereas it is consistently low at night.

Next to abundance we also measured ground speeds and flight directions. Throughout the year, observed ground speeds were slightly higher during the night than during the day, and in spring and winter relative to summer and autumn. These differences can be caused by differences in species composition, flight behaviour, and amount of wind support. However, further knowledge about species distribution and flight behaviour would be required to confirm this. Outside of nocturnal migration, observed flight directions were mainly towards the south and south-east. This was unexpected, as we assumed we would observe a more uniform distribution of directions or bimodal distributions of birds commuting out to sea and back. Possibly birds flying out from the coast do so at a different altitude due to differences in wind support and will therefore not be detected easily by the horizontal radar. Alternatively, there might be an unexpected bias of the radar for observing birds flying in a specific direction. Further investigation is needed to find out whether this pattern is due to a bias in radar observations or bird behaviour.

We investigated nocturnal migration in spring and autumn more in-depth. Several high-intensity migration nights occurred within the study period, mostly during autumn migration. In autumn, we observed more high intensity migration nights than in spring, as adverse weather conditions might limit the number of nights suitable for migration. In autumn, the period of intense migration (last week in September – early November) strongly overlapped with findings in the region using military radar in 2006-2008 (Shamoun-Baranes and van Gasteren 2011). In both seasons, most observed birds flew at low altitudes and within rotor height of Gemini wind park. The initial Environmental Impact Assessment considered the collision risk for migratory birds very small (Burggraaf-van den Berg et al. 2012), but noted further monitoring was required. We show that MTRs can be relatively high during nights of intense migration, similar to hourly peaks observed in Luchterduinen wind farm (Bradarić et al. 2022), and flight altitudes overlap with the rotor swept zone to a large extent. Therefore, we estimate bird-wind farm interactions are considerable during nights of intense migration and migratory movements should be taken into account for future wind farm developments in the region.

During this project we developed tools for post-processing bird radar data which gave us more reliable results. Field validation of radar measurements is an important factor in this process (van Erp et al. 2024, available in Appendix 3). The field validation at Gemini wind park was used to confirm several of the species flying in the area. Unfortunately, the high sea-state during most observation days prevented us from validating the radar tracks themselves, mostly because there was a large overlap between observation area and the area close to the radar which is filtered out. Therefore, future validation studies should ideally be carried out at a distance of 1000-2000m from the radar position. This way, the observation field of view overlaps with the area of the radar in which bird detectability is highest. The high sea-state also resulted in periods of time in which reliable bird measurements were impossible. Especially in winter, where weather conditions often prevent accurate radar measurements, this caused in a relatively low amount of available observation hours. To address this limitation, long-term and continuous and data storage is vital, as this is the only way we can overcome gaps in the data and discern general patterns of bird flight. For example, without several years of data we would not have been able to discern daily and seasonal flight patterns in winter or get a good overview of high-intensity nocturnal migration in spring and autumn. Maintaining the data infrastructure to allow for these long-term data collection scheme should therefore be a priority for biodiversity monitoring in relation to wind energy.

# 8. Research outcomes

The data and insights gained during this project directly or indirectly contributed to the following scientific publications:


- Bradarić M, Bouten W, Fijn RC, Krijgsveld KL, Shamoun–Baranes J (2020) Winds at departure shape seasonal patterns of nocturnal bird migration over the North Sea. Journal of Avian Biology 51:jav.02562.
- Manola I, Bradarić M, Groenland R, Fijn R, Bouten W, Shamoun-Baranes J (2020) Associations of Synoptic Weather Conditions with Nocturnal Bird Migration Over the North Sea. Frontiers in Ecology and Evolution 8:542438.
- van Erp J, Sage E, Bouten W, van Loon E, Camphuysen K, Shamoun-Baranes J (2023) Thermal soaring over the North Sea and implications for wind farm interactions. Marine Ecology Progress Series 723:185-200.
- Van Erp JA, van Loon EE, Camphuysen KJ, Shamoun-Baranes J (2021) Temporal patterns in offshore bird abundance during the breeding season at the Dutch North Sea coast. Marine Biology 168:150.
- van Erp JA, van Loon EE, De Groeve J, Bradarić M, Shamoun-Baranes J (2024) A framework for post-processing bird tracks from automated tracking radar systems. Methods in Ecology and Evolution 15:130-143.

## Acknowledgements

We thank Maja Bradarić for her support with identifying migration and calculating mean traffic rates. Maja Bradarić and Johannes De Groeve developed the scripts for querying and post-processing the vertical radar data. Additionally, Johannes De Groeve provided support for all other steps of accessing and post-processing the radar data. We thank SURFsara for the collaborative effort for storing the data. This work benefits greatly from the ongoing collaboration between Robin Radar, Waardenburg Ecology, and Rijkswaterstaat, to help better interpret the radar data.

## Funding

This study and the project "Spatial and temporal dynamics of bird movement over the North Sea" (GEM-03-266) was funded by Gemini wind park, and additionally supported through the Open Technology Programme, project "Interactions between birds and offshore wind farms: drivers, consequences and tools for mitigation" (project number 17083), which is financed by the Dutch Research Council (NWO) Domain Applied and Engineering Sciences, in collaboration with the following public and private partners: Rijkswaterstaat and Gemini wind park. The use of the national computer facilities in this research was subsidized by NWO Domain Science with the support of SURF Cooperative.

## Appendices

All appendices are available on figshare (https://doi.org/10.21942/uva.25021793).

- Appendix 1: The post-processing, analysis and visualization R-scripts for Gemini report 03-266.
- Appendix 2: All research articles listed in Chapter 8 "Research outcomes".
- Appendix 3: Leemans JJ, Bravo Rebolledo EL (2023) Bird radar observations in offshore wind farm Gemini. Report 18-0610.

# References


- Bradarić M (2022) On the radar: weather, bird migration and aeroconservation over the North Sea. University of Amsterdam
- Bradarić M, Bouten W, Fijn RC, Krijgsveld KL, Shamoun–Baranes J (2020) Winds at departure shape seasonal patterns of nocturnal bird migration over the North Sea. Journal of Avian Biology 51:jav.02562.
- Burggraaf-van den Berg I, Argiolu R, Verlinde Y (2012) MER windparken Gemini Deel A. Arcadis Nederland BV, Arnhem.
- De Groeve J (2023) AME Infrastructure Manuals. Gitlab repository, https://gitlab.com/uva_ibed_ame/ame-infrastructures-manuals.
- De Groeve J, van Erp J (2023) birdR. https://gitlab.com/uva_ibed_ame/robin_radar/birdar.
- Dierschke V, Furness RW, Garthe S (2016) Seabirds and offshore wind farms in European waters: Avoidance and attraction. Biological Conservation 202:59–68.
- Fijn RC, Arts FA, de Jong JW, Beuker D, Bravo Rebolledo EL, Engels BWR, Hoekstein MSJ, Jonkvorst R-J, Lilipaly S, Sluijter M, van Straalen KD, Wolf PA (2018) Verspreiding en abundantie van zeevogels en zeezoogdieren op het Nederlands Continentaal Plat 2017-2018. Bureau Waardenburg & Delta Project Management.
- Fijn RC, Gyimesi A (2018) Behaviour related flight speeds of Sandwich Terns and their implications for wind farm collision rate modelling and impact assessment. Environmental Impact Assessment Review 71:12–16.
- Jonker SI, Kouwenberg AMC, Salomons MC, Snoek RC, van der Zon SPE (2012) Passende beoordeling windparken en kabeltracé Gemini. Arcadis Nederland BV, Apeldoorn
- Leemans JJ, Bravo Rebolledo EL (2023) Bird radar observations in offshore wind farm Gemini. Waardenburg Ecology.
- Manola I, Bradarić M, Groenland R, Fijn R, Bouten W, Shamoun-Baranes J (2020) Associations of Synoptic Weather Conditions with Nocturnal Bird Migration Over the North Sea. Frontiers in Ecology and Evolution 8:542438.
- Qi J, Shamoun-Baranes J (2024) An architectural roadmap for a national e-science infrastructure for remote monitoring of avian movement. University of Amsterdam, Amsterdam, doi: https://doi.org/10.21942/uva.25011845.
- Sage E, Shamoun-Baranes J (2022) Offshore space use of lesser black-backed gulls Larus fuscus from the Schiermonnikoog breeding population. Report No. 22-40-107. University of Amsterdam.
- Sage E (2022) Wind energy for all! The dynamic flight of gulls in human-engineered landscapes. University of Amsterdam.
- Shamoun-Baranes J, van Loon E, Liechti F, Bouten W (2007) Analyzing the effect of wind on flight: pitfalls and solutions. Journal of Experimental Biology 210:82–90.
- Shamoun-Baranes J, van Gasteren H (2011) Atmospheric conditions facilitate mass migration events across the North Sea. Animal Behaviour 81:691-704.
- Shealer DA (2002) Foraging behavior and food of seabirds. Biology of Marine Birds 137-177. CRC Press.
- Spear LB, Ainley DG (1997) Flight speed of seabirds in relation to wind speed and direction. Ibis 139:234–251.
- van Bemmelen RSA, Geelhoed SCV, Leopold MF (2015) Gemini T-0: local seabirds. IMARES Wageningen UR.
- van Erp J, Sage E, Bouten W, van Loon E, Camphuysen K, Shamoun-Baranes J (2023) Thermal soaring over the North Sea and implications for wind farm interactions. Marine Ecology Progress Series 723:185-200.
- van Erp JA, van Loon EE, Camphuysen KJ, Shamoun-Baranes J (2021) Temporal patterns in offshore bird abundance during the breeding season at the Dutch North Sea coast. Marine Biology 168:150.
- van Erp JA, van Loon EE, De Groeve J, Bradarić M, Shamoun-Baranes J (2024) A framework for post-processing bird tracks from automated tracking radar systems. Methods in Ecology and Evolution 15:130-143.

## Supplementary material

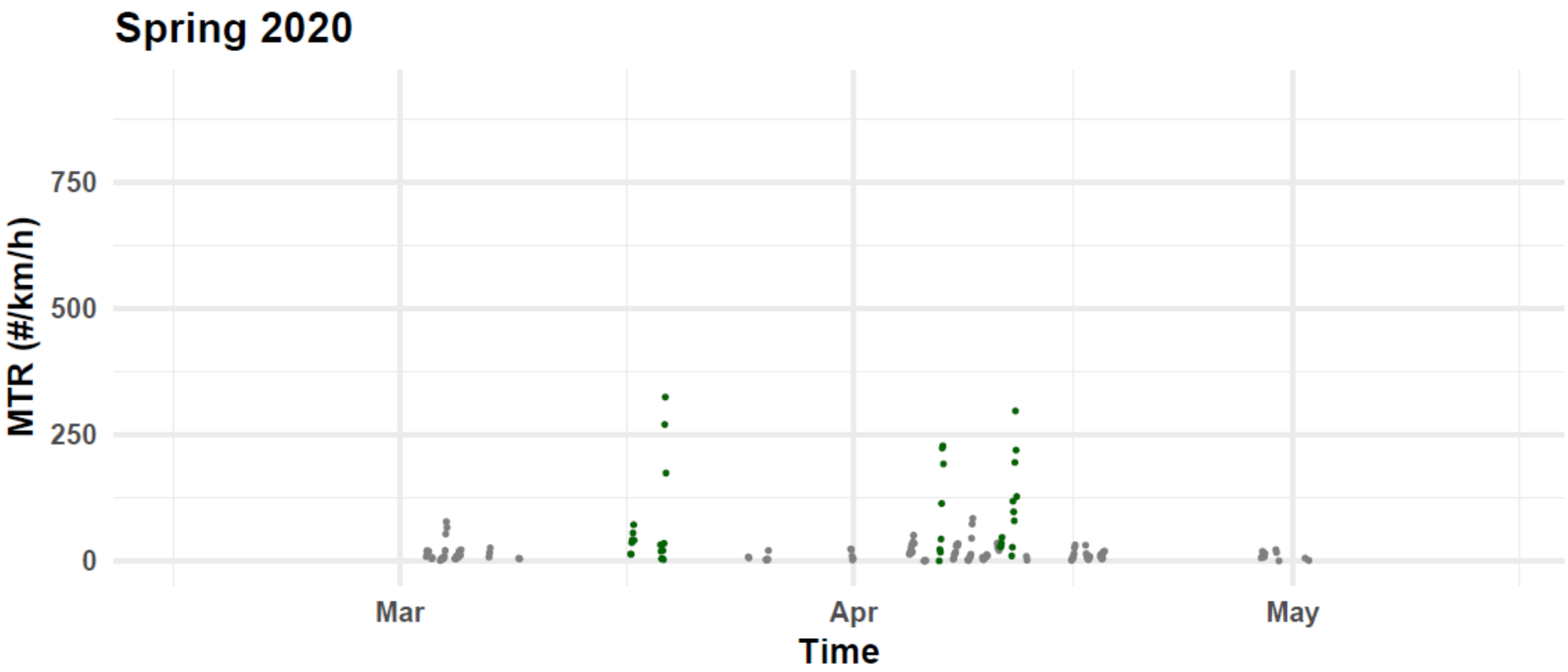


Supplementary Figure 1. Houry MTR (birds $km^{-1}$ $h^{-1}$) for all nights in spring 2020. MTRs in nights of intense migration (based on the average MTR throughout the night) are depicted in green.

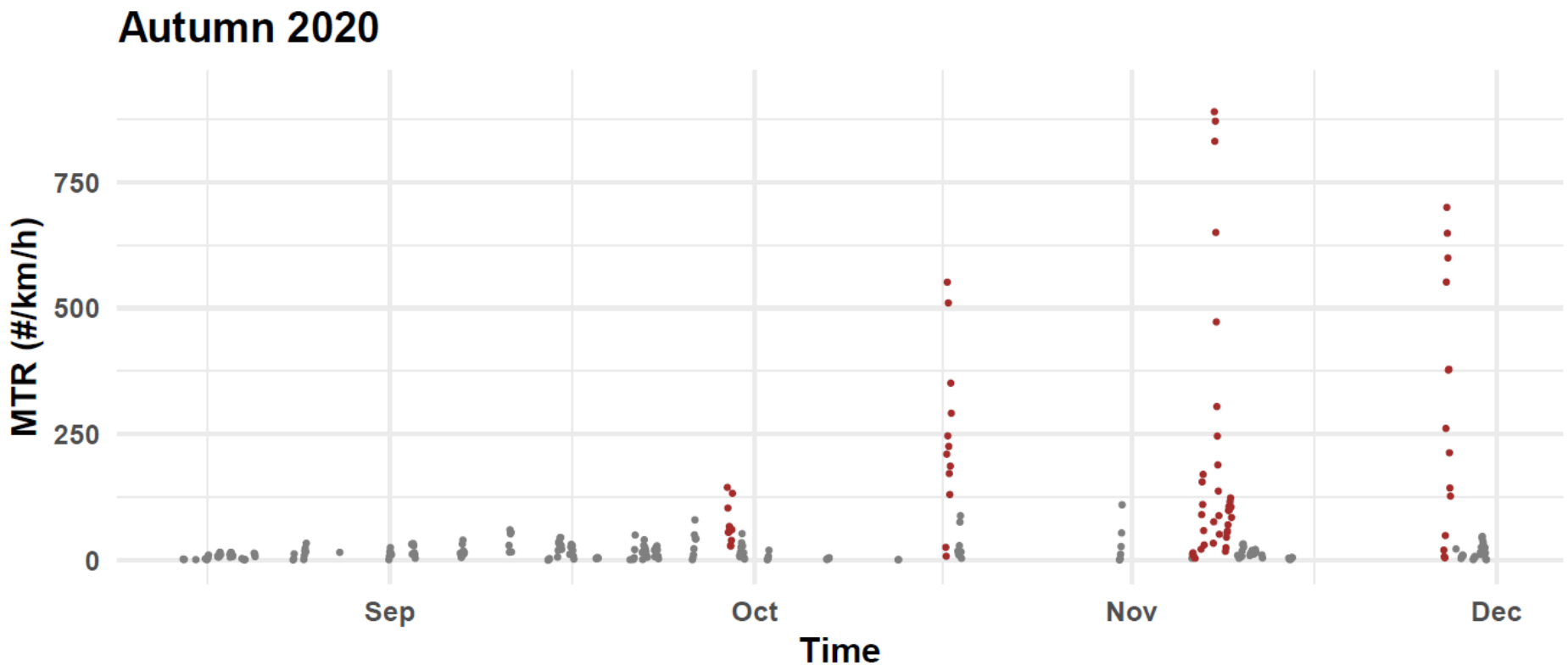


Supplementary Figure 2. Houry MTR (birds $km^{-1}$ $h^{-1}$) for all nights in autumn 2020. MTRs in nights of intense migration (based on the average MTR throughout the night) are depicted in brown.

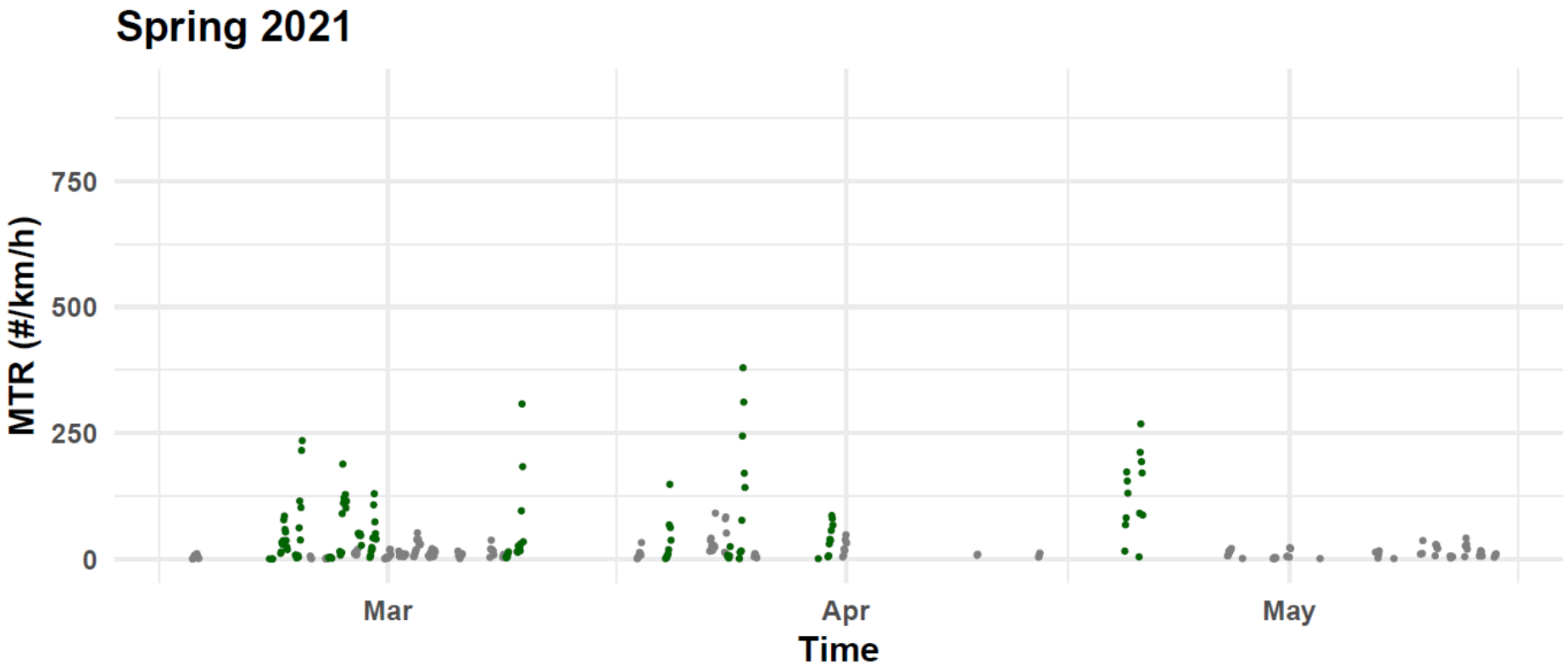


Supplementary Figure 3. Houry MTR (birds $km^{-1}$ $h^{-1}$) for all nights in spring 2021. MTRs in nights of intense migration (based on the average MTR throughout the night) are depicted in green.

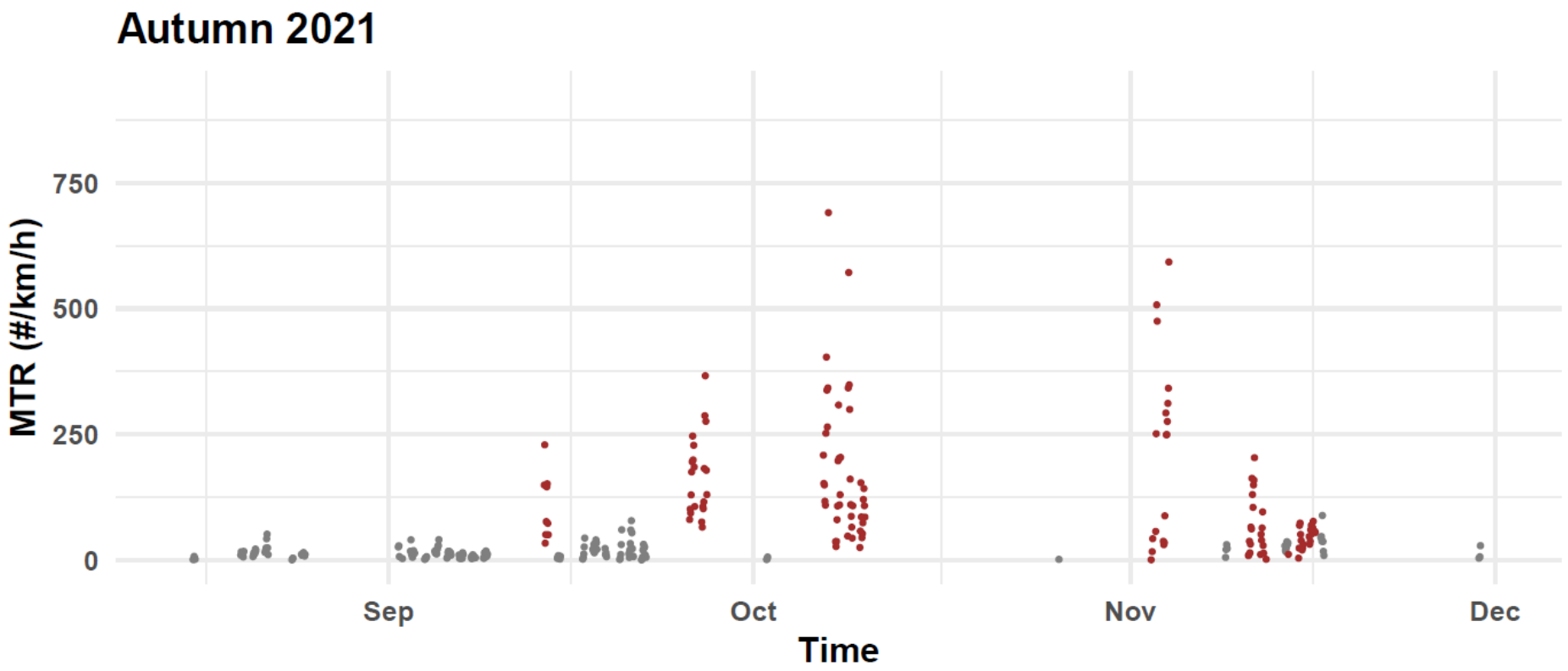


Supplementary Figure 4. Houry MTR (birds $km^{-1}$ $h^{-1}$) for all nights in autumn 2021. MTRs in nights of intense migration (based on the average MTR throughout the night) are depicted in brown.

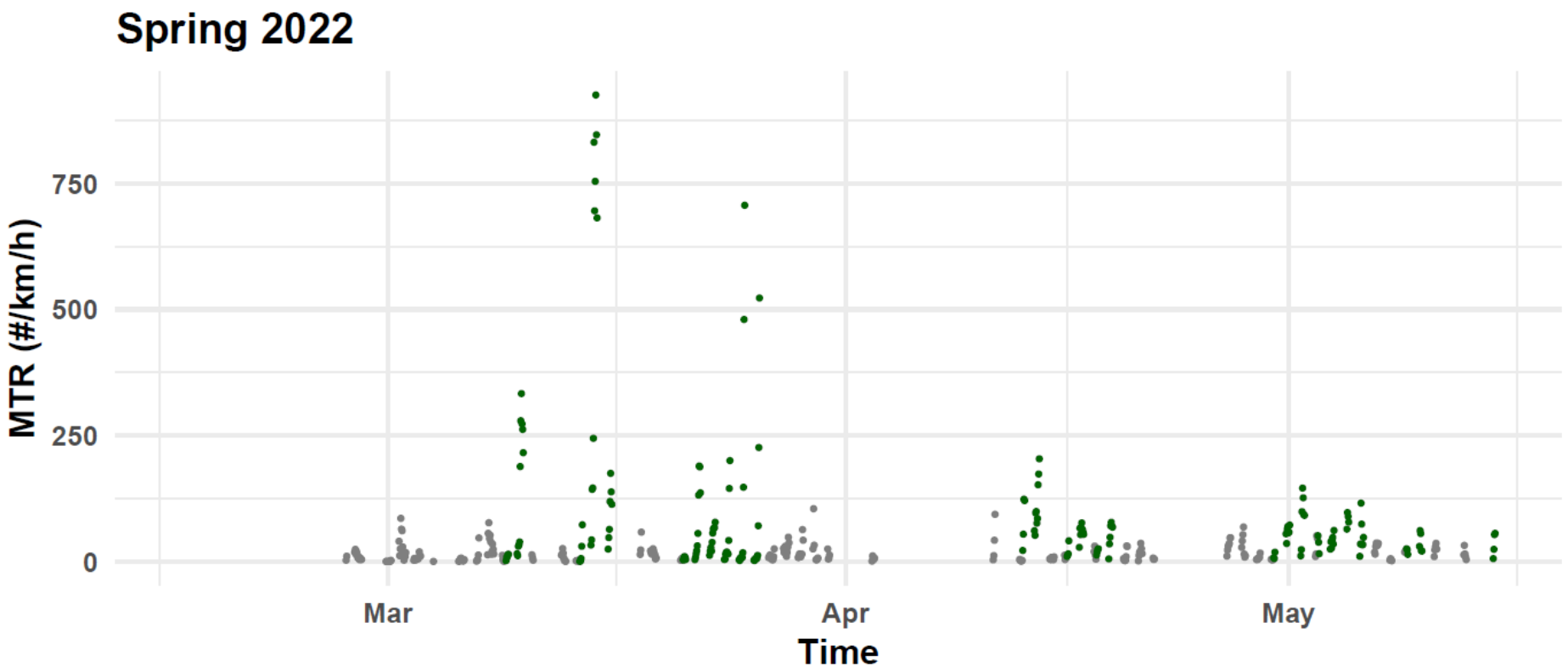


Supplementary Figure 5. Houry MTR (birds $km^{-1}$ $h^{-1}$) for all nights in spring 2022. MTRs in nights of intense migration (based on the average MTR throughout the night) are depicted in green.

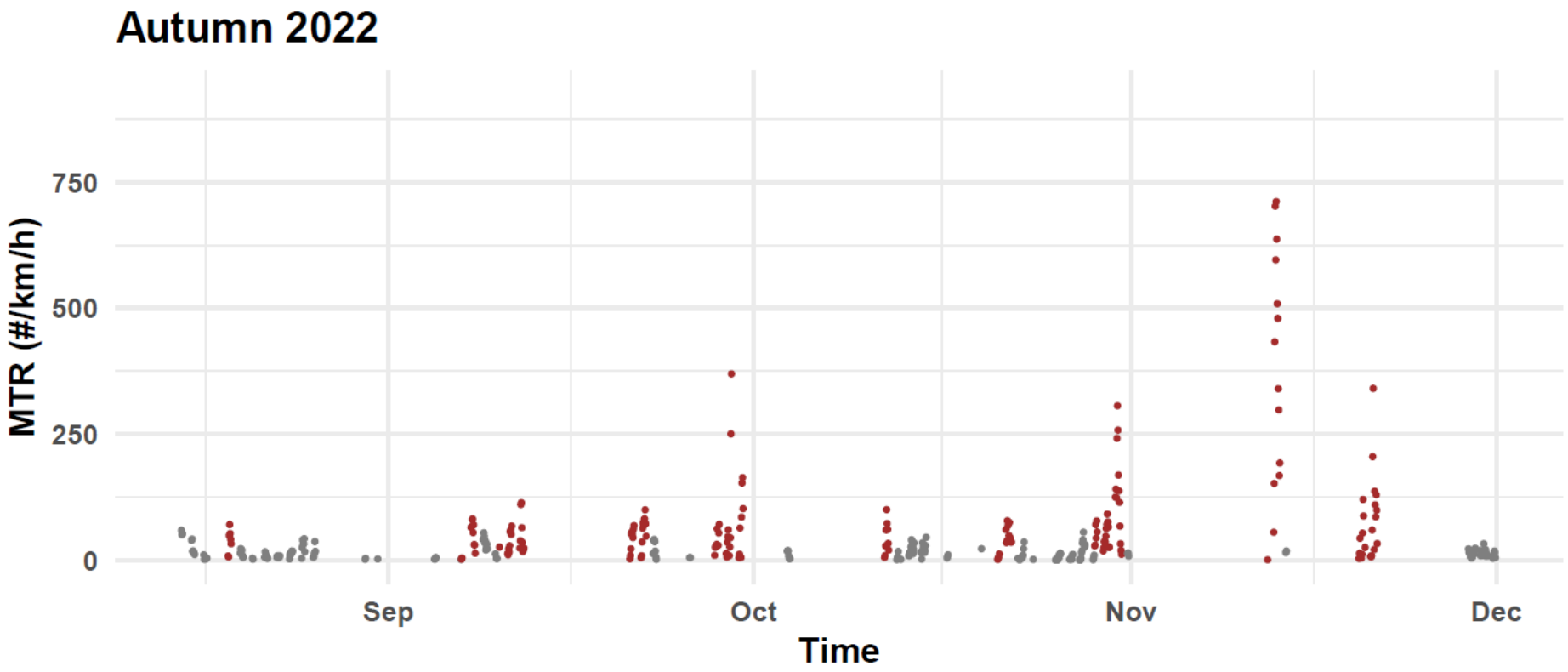


Supplementary Figure 6. Houry MTR (birds $km^{-1}$ $h^{-1}$) for all nights in autumn 2022. MTRs in nights of intense migration (based on the average MTR throughout the night) are depicted in brown.